CHAPTER 12 – VERTICAL AND LATERAL SEISMIC PROFILES

R.C. Hinds, (Coordinator), Department of Geology, University of Pretoria;

R.D. Kuzmiski, Computalog Gearhart Ltd.;

W.J. Botha, Department of Geology, University of Pretoria;

N.L. Anderson, Department of Geological Sciences, Ohio University.

INTRODUCTION

During recent years, vertical seismic profiling (VSP) and lateral seismic profiling (LSP) have evolved into viable exploration tools. As shown in Figure 12.1, these methods involve the recording of seismic energy using the geophones placed inside the well borehole. Operationally, the geophones are contained in a well sonde that is lowered to the bottom of the borehole. As the tool is lowered, check-depth VSP recordings are done at intervals of 500 m or so. These VSP recordings will be used to check with recordings made at the same wireline depth level when the tool is later raised up the borehole as a check for the detection of cable stretch or wireline depth gauge malfunction. When the geophone sonde reaches the bottom of the borehole, the wireline truck raises the sonde to the first depth location beginning production VSP recordings. The sonde has a locking arm that forces the geophone assembly against the wall of the open borehole or casing. During each reading, the sonde is locked to the wall and then released while being raised to the next location. Unlike the check shot survey, these methods record the seismic energy beyond the time of the first break energy reaching the tool. Utilizing the first break energy and subsequent recordings, the interpretation of the dataset takes on a very different nature from surface seismic. The interpretation of VSP's and LSP's is the topic of this chapter. Abbreviations used in the text are given in Table 12.1.

VSP's and LSP's have been used to delineate both carbonate and clastic reservoirs. Interpreted LSP data have encouraged and, at other times, discouraged whipstock drilling in the rapid turnaround time required to meet oil companies' demands. Higher-frequency

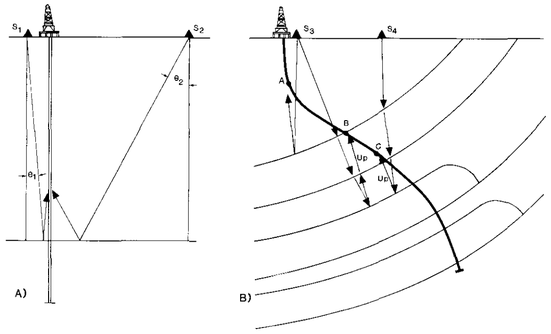

Figure 12.1. The field layout of the VSP and the LSP. In part (A) the source at S_1 is a zero-incidence location with respect to geophones in the vertical non-deviated borehole. The downgoing and upgoing waves travel vertically down to the reflector and back to the receiver geophone in the borehole. The source at S_2 is a non-zero offset location as the source does not lie directly over the geophone. In part (B) in the deviated hole source S_3 is in a zero-offset configuration for the upper vertical part of the hole and a non-zero offset for the deviated remainder of the borehole. Source S_4 approximates a zero-offset location. Part (B) is usually represented in the literature as a deviated borehole intersecting horizontal layers. This would yield incorrect reflection angles for the migration algorithms.

Table 12.1. Abbreviations used within the text in order of appearance

ABBREVIATION	DESCRIPTION
VSP	Vertical Seismic Profile
LSP	Lateral Seismic Profile
IPP	Interpretive Processing Panel
IIP	Integrated Interpretive Display
FRT	Field Recorded Time
+TT	First break times are added to each respective trace
-TT	First break times are subtracted from each respective trace
HMIN, HMAX	Output rotation channel using X and Y data using downgoing P-wave hodograms
HMAX', Z'	Output rotation channel using Z and HMAX data using downgoing P-wave hodograms
$HMAX'_{up}$, HMAX'down	Outputs of HMAX' channel after wavefield separation of up and downgoing waves
Z'up, Z'down	Outputs of Z' channel after wavefield separation of up and downgoing waves
Z_{up}, $HMAX_{up}$	Outputs of Z'_{up} and $HMAX'_{up}$ after de-rotation
Z''_{up}, $HMAX''_{up}$	Outputs of Z_{up} and $HMAX_{up}$ after time-variant model-based rotations
VSPCDP	transformation from depth and pseudo two-way traveltime to offset away from the well and pseudo two-way traveltime

upgoing wavefield data have provided explorationists with a more detailed understanding of subsurface morphologies (Hardage, 1983; Balch and Lee, 1984; Balch et al., 1981; Kennett et al., 1980). The interpretation of far-offset LSP's, when the triaxial geophone data is orthogonally rotated into P, SH and SV wavefield components by specialized processing techniques, to be discussed in this chapter, have aided in the delineation of clastic reservoirs by comparing each component's attenuation properties in the media of interest. Unfortunately, very few interpretation examples from the Western Canadian Sedimentary Basin have appeared in the literature.

The interpretation of the VSP's and LSP's is intimately linked to the processing of these data and to their integration with the other exploration information such as dip-meter results, gamma-ray logs, sonic logs and surface seismic data. In order to assure optimal use of this integrated dataset, the explorationist must evaluate the effect of the various processing steps on the data. A processing and display sequence, herein referred to as interpretive processing panels (IPP) is developed (Table 12.1). This system enables an interpreter to monitor each step of the processing and to delineate selected seismic markers on the raw through to the final processed data. The causes of anomalies on the VSP or LSP data, either processing or geology, can best be evaluated using these panels.

The geometry for the VSP consists of an energy source placed vertically or approximately vertically above the sonde (making a

ACKNOWLEDGEMENTS

We would like to thank and recognize Gulf Canada Ltd. and Petro-Canada Inc. of Calgary for the data in this project. We would like to thank Dr. J.V. Pendrel of Gulf Canada Ltd. for reviewing the text. This chapter is part of a Ph.D. thesis being pursued by the chapter co-ordinator, R.C. Hinds. The data was prepared and processed at Inverse Theory and Applications Inc., Computalog Gearhart Ltd. and B.P. Canada Ltd.

near-zero angle between vertical, sonde and source) in the borehole. This type of geometry is referred to as a zero or near offset VSP. However, when the source is not directly above the sonde but is offset horizontally forming an appreciable non-zero angle between the vertical, sonde and source, then the method is called a non-zero offset LSP. This definition of the LSP also applies in a deviated borehole where the source is at the wellsite but the sonde is horizontally displaced from being vertically under the wellsite (Fig. 12.1).

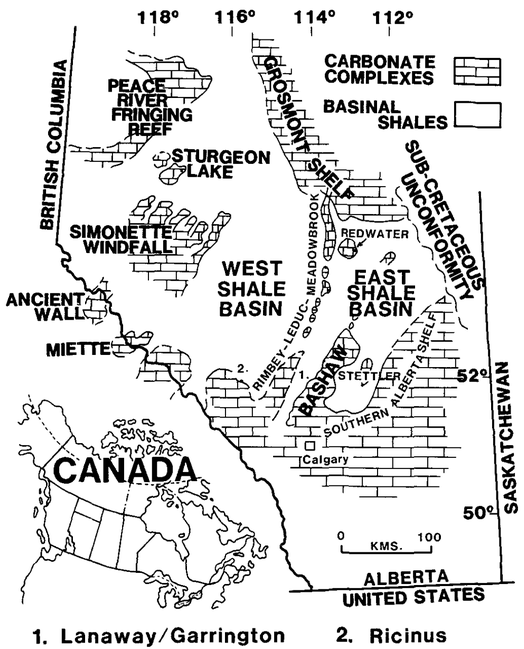

Figure 12.2. Map of Alberta showing the various Woodbend reef features. The Lanaway/Garrington and Ricinus examples are labelled example 1 and 2.

The objective of this chapter is to discuss the interpretation of VSP and LSP data using two case histories (Fig. 12.2). Both datasets were acquired for Leduc Fm plays (Chapter 4). The IPP (interpretive processing panels) are displayed for the VSP dataset from the Lanaway/Garrington and the Ricinus areas (Fig. 12.2). The Lanaway/Garrington VSP data is merged with well-log and surface seismic data in another interpretive display referred to as the integrated interpretive display (IID). The use of the LSP data to evaluate subsurface structure away from the borehole is discussed in the LSP example from the Ricinus field (Fig. 12.2).

VSP's can be thought of as modified check-shot surveys. However, unlike the check-shot survey where only the first breaks are recorded, in the VSP the geophones in the borehole record both up and downward travelling waves (Fig. 12.3) for several seconds

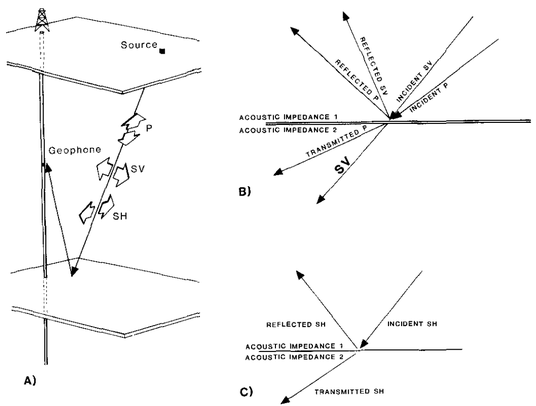

Figure 12.3. The downgoing and upgoing waves (upgoing wave shown in part A) propagating to the wellbore geophone tool can be compressional P waves that vibrate in the direction of travel or Shear SV or SH waves that vibrate normal to the direction of travel, either in the plane of the source and receiver or out of the plane. Reflections from dipping and contorted geological strata can enable all three of these type wavefields to be recorded on the X,Y and Z geophones. At impedance interfaces the P and SV waves can reflect and transmit as P or SV waves (B). The SH incident wave reflects and transmits as an SH wave (C).

after the first arriving energy reaches that downhole geophone location. Unlike a surface seismic survey where the geophones are placed on the ground surface and receive only upgoing waves, the VSP geophones receive upgoing waves from reflections originating below, and also the downgoing waves that are transmitted directly to or reflected down to the geophones (Fig. 12.3). Any downgoing waves that arrive after the first break (the primary downgoing wave) can be either P to SV mode converted downgoing primary waves, SV downgoing primary waves (generated at or near the source) or reflected P or SV downgoing wave multiples (Fig. 12.3). The primary P to SV mode converted downgoing waves arrive later in time and at a *deeper geophone location than the primary non-converted P wave* due to the lower SV wave velocity and altered angle of transmission at the point of conversion.

Upgoing and downgoing waves are sketched in the ray-path diagram in Figure 12.4a. As illustrated, downgoing multiples arrive later than the downgoing primary waves. The corresponding traveltime curves are shown in Figure 12.4b. Note that the upgoing and downgoing waves trend in opposite directions on the depth/traveltime plot.

As the geophone is lowered into the borehole:

1) the traveltime of the upgoing waves decrease since the downward travelling geophone is travelling towards the geological reflector (Fig. 12.4);

2) upgoing reflections from a particular horizon will cease to be recorded when the geophone is deeper than that horizon (Fig. 12.4);

3) the upgoing primary reflected waves will merge with the primary downgoing wave on the VSP depth/traveltime plot where the geophone intercepts the reflecting horizon (Fig. 12.4);

4) the traveltime of the downgoing primary wave will increase (Fig. 12.4); and

5) the traveltimes of the downgoing surface-generated multiples and interbed multiples will increase. The surface generated multiples will appear on the data from the shallowest recorded *geophone level to the deepest level and will be a delayed ghost* of the downgoing primary. The interbed downgoing multiple will be recorded only where the geophone is beneath the TOP

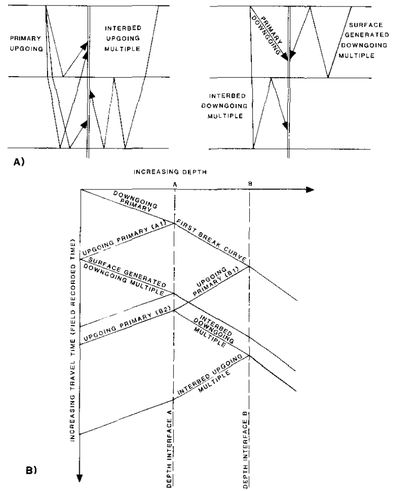

Figure 12.4. Examples of the upgoing and downgoing raypaths for both primary and multiple reflections are shown in part A. The upgoing rays are illustrated on the left side of the diagram whereas the downgoing rays are illustrated on the right side. The geometry for the zero-offset sources are displayed with exaggerated source offset for clarity. The surface generated downgoing multiples will be recorded at all subsurface geophone locations whereas the interbed downgoing multiple generated between layers A and B will only be recorded when the geophone is below layer A. Upgoing reflections from layer A will be recorded only at geophone locations above layer A. The up and downgoing primaries will merge when the geophones are located at the generating interface. A traveltime curve plot for the up and downgoing rays is shown in part B. The downgoing primary is the first break curve increasing in time from left to right in the diagram and with the exception of head waves is the first recorded signal on each VSP trace. The downgoing wave multiple for the zero-offset case parallel the downgoing primary. An upgoing primary (B1) generates a reflected downgoing multiple at interface A, which in turn can generate an interbed upgoing multiple at reflector B.

layer that generates the downgoing reflection of the multiple. Above that layer, the interbed downgoing multiple is not recorded (Fig. 12.4) as a downgoing wave.

Compressional (P), shear vertical (SV) and the shear horizontal (SH) ray-paths are depicted in Figure 12.3. Depending upon the emergent angles that the various modes have with the X,Y and Z axis of the geophone package (Fig. 12.5), these wavemodes will be vectorially partitioned between the three downhole geophone axes. The result is that the Z-axis geophone will not record P wave energy only but will record a combination of P and SV energy. Similarly the X- and Y-axis geophones will record some P-wave energy. Figure 12.5 illustrates that the amount of partitioning onto the various axes

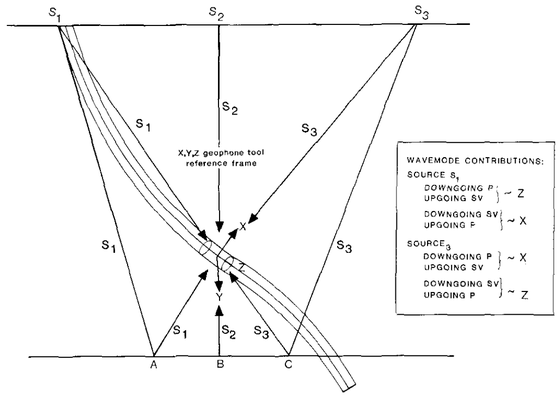

Figure 12.5. For the deviated borehole in the diagram, the triaxial geophone package will receive contributions of P, SV and SH waves on all geophone axis. The Z component even for the "zero-offset" source location at S2 will not contain P waves only. To separate the various wavefield contributions, the geophone package will be numerically rotated using hodogram polarization analysis (Fig. 12.24). This is the "theoretical" geometry used in the analysis of the upgoing rays for the deviated borehole. Note however that the upgoing rays travel very different directions when the subsurface layers are not horizontal as in Figure 12.1.

can vary significantly depending on the source-receiver geometry in the deviated borehole example.

The three geophones in the triaxial sonde are oriented vertically and horizontally with the two horizontal geophones aligned orthogonal to each other. Usually, there will be three geophones aligned in series in each direction for a total of nine geophones per tool. As the sonde with the triaxial geophone package is lowered down the borehole (Fig. 12.5), the VSP tool containing the geophone package will rotate and the X and Y channels will change orientation due to the twisting motion of the wireline cable and the deviation of the borehole. In the processing sequence, various numerical pseudo-rotations are needed to redistribute the P, SV and SH energy back onto separate channels. These numerical rotations or redistributions of the recordings from the three geophone axis onto new orientation axis are called the polarization or hodogram analysis and a recent development called time-variant model-based polarization. These two methods will be discussed in the far-offset LSP case history.

ZERO OFFSET CASE HISTORY

REGIONAL GEOLOGY AND GEOPHYSICS

The VSP example for the Lanaway/Garrington area is a zero-offset dataset. In Figure 12.2 the approximate location of the well is shown. The primary geological target is the updip edge of a gas prone Leduc Fm reef. This Leduc Fm reef is approximately 200 m high with an updip eastern edge containing a 50 m pay zone. The eastern and western limits of the gas pool are the reef fore-slope and the gas-water interface, respectively.

The main pre-drilling seismic interpretation markers are displayed on the surface seismic line shown in Figure 12.6. A time-structural anomaly at the Leduc level near the well location is interpreted as localized Leduc structure. This time-structural anomaly is associated with both a character and isochron change. Specifically, near the well location the Leduc event broadens into two peaks, the upper of which was interpreted as the top of a localized structure on the otherwise relatively flat reef. The Leduc to Cretaceous, Leduc to Wabamun and the Leduc to Cambrian isochrons were also interpreted as indicative of a thicker buildup.

Drilling, on the basis of the interpretation of the surface seismic data, was expected to show the overlying Ireton to be as thin as 10

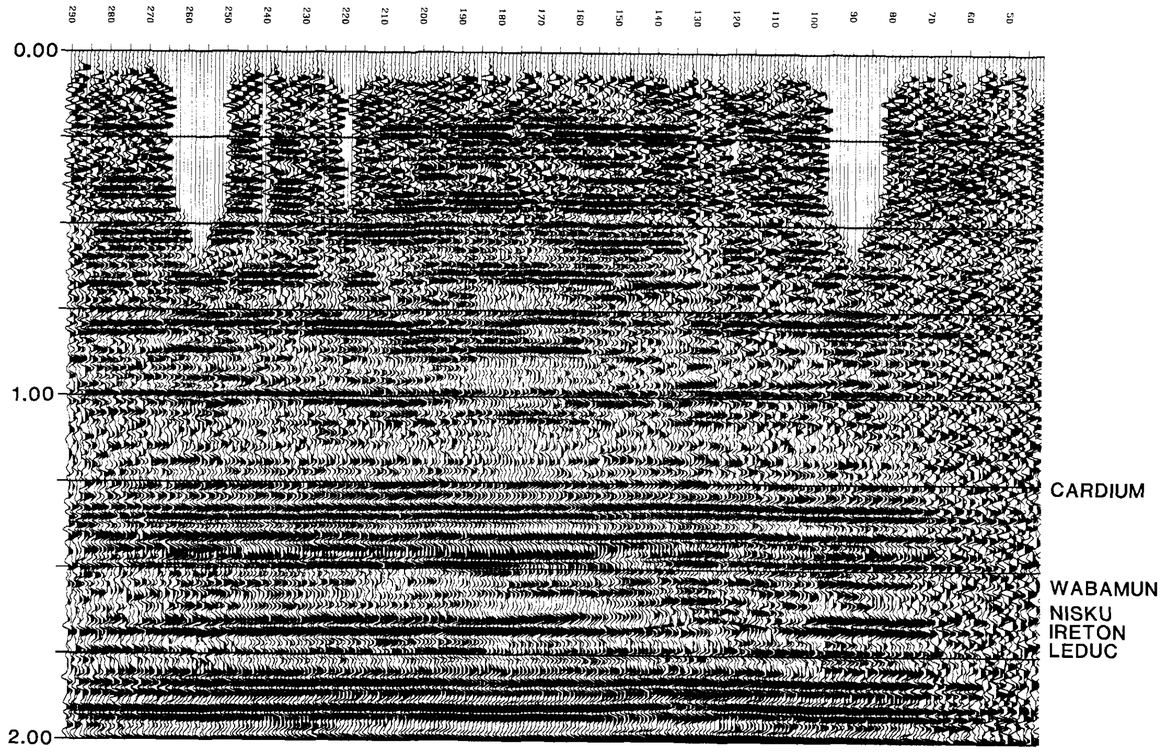

Figure 12.6. The pre-drilling interpretation of the surface seismic line over the Lanaway/Garrington well. The interpreted seismic markers are Cardium Fm, Wabamun, Nisku, Ireton and Leduc formations. The interpreted localized Leduc Fm anomaly is structurally 25 ms above the main Leduc reef event.

m. However, the Ireton Fm was no thinner at the proposed well location than in neighbouring wells to the west and north. Economically, however, there was a greater gross pay section suggesting that the Leduc Fm here had been structurally uplifted by some 30 to 40 m. The gas/water contact differed from the neigbouring wells to the north so that the well location was classified as a separate pool.

The VSP was run in order to resolve the discrepancy between the interpreted surface seismic data and the well data. Specifically, the interpretation of the VSP was expected to determine:

1) the nature of the character anomaly on the seismic data; and

2) the isochron/isopach relationship of the anomaly.

SEPARATION OF UPGOING AND DOWNGOING WAVES

In the following text, the terms FRT, +TT time and -TT time will be used repeatedly (Table 12.1). When the data are recorded in

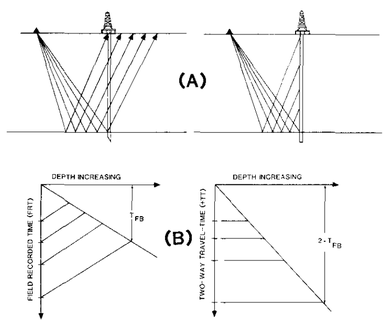

Figure 12.7. Part (A) shows the geometry of the surface seismic with the well superimposed on the raypaths. To the right, the rays that are terminated at the well are different from the surface seismic rays by a traveltime equivalent to the zero-offset first break times of the downgoing rays. In part (B) when the first break traveltimes are added back onto the traces, the time axis changes from field recorded time to two-way traveltime (+TT) that should be equivalent to the surface seismic two-way traveltime axis.

the field without any bulk shift being added or subtracted from the raw recorded times, the term FRT (field recorded time) is used to describe the time placement of the data. To align the data along the first break picks, the first-break traveltime for each trace is subtracted from that trace and the aligned data is bulk shifted to some time datum (usually to 100 or 200 ms). The data in that configuraton is said to be in -TT time (the TT refers to the first break traveltime for that trace). To align the upgoing waves of a zero-offset VSP (imaging flat interfaces) horizontally, each trace's respective first break time is added to that trace. The data in this time configuration is said to be in +TT time.

To evaluate data quality during interpretation, the effects that various processing operations have on the raw through separated upgoing P wave data, must be systematically analyzed. It is the upgoing waves, placed into pseudo-two-way time (+TT), that are directly tied to the surface seismic at the wellbore location (Fig. 12.7). Unfortunately the upgoing waves are always of significantly lower amplitude than the downgoing waves. If these weaker upgoing waves are distorted during processing then this operation should be followed back to where these waves are interpreted to be distorted and reprocessed from that point on.

The IPP in Figure 12.8 consists of seven panels which depict the raw data through to the wavefield separated data. The first and second panels show the raw and gained data in field recorded time (FRT). These two plots allow for an evaluation of the relative signal power of the upgoing and downgoing wavefields. Note the difference between the amplitudes of the upgoing and downgoing waves where they constructively and destructively interfere in the area of the first break (Fig. 12.8, panel 1). If the downgoing wave contamination is too severe then the various processing steps that analyze the data in the first break zone such as wavefield separation will be suspect. The primary events have been interpreted on the entire set of panels. In Figure 12.8, shallow interbed multiples are also interpreted.

The wavefield separation quality control panels are displayed as panels 3, 4, 5 and 6 in Figure 12.8. In order to separate the upgoing and downgoing waves, the downgoing waves are aligned horizonatally and enhanced by median filtering in panel 4. Panel 4 is then subtracted from the combined wavefield panel (in -TT) of panel 3 to yield the upgoing wavefield display of panel 5. The separated upgoing waves are shown in two-way traveltime (+TT) without and with an application of a median filter in panels 6 and 7, respectively. The sequence of panels 3 to 6 show that the wavefield separation operation has not significantly altered the signal information contained in the separated upgoing waves.

The initial interpretation of the upgoing events is performed using the median filtered separated upgoing waves in (+TT) time (Fig. 12.8, panel 7). This interpretation is incorporated into the previous panels in Figure 12.8. The zero-offset VSP interpretation is premised on the basis that only primary VSP events intersect the first break curve (an upgoing wave reflecting from a boundary merges with the downgoing primary when the geophone is at that interface). As the depth of the seismic markers is known from drilling, the trace for that particular depth can be determined and then followed to the first break. At that first break point, the corresponding primary upgoing event will be observed.

The wavefield (up and downgoing waves) separation in Figure 12.8 was performed with the use of median filtering. There are other methods of wavefield separation such as Karhunen-Louve method, the wave equation based methods, the frequency-wavenumber method and the Tau-P method. A comparison of all of the methods with respect to interpretation is a topic for future research.

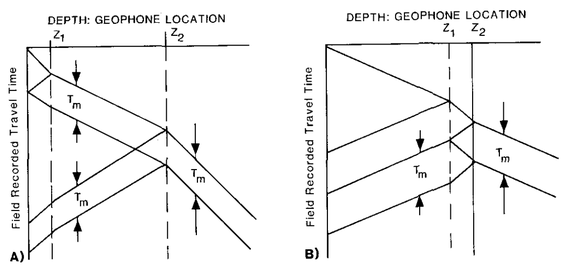

Figure 12.9. Analogous to Figure 5-32 of Hardage (1983), part (A) shows the depth verus FRT configuration for the surface generated multiple. The numerical operator (inverse filter) that attenuates the downgoing multiple (the downgoing wave that is time shifted from the primary downgoing wave by time Tm) will attenuate the upgoing surface generated multiple. In part (B) the operator that will attenuate the upgoing interbed multiple can be designed from any trace recorded beneath depth location Z1.

DECONVOLUTION PANELS

The downgoing waves contain the surface generated and interbed multiples that appear on both upgoing VSP and surface seismic data. The separated downgoing wavefield can be deconvolved to a single primary pulse using an inverse filter operation. The filter is designed from the downgoing wave panel (Fig. 12.8, panel 4) so that all relevant multiples can be represented and therefore collapsed. That same deconvolution filter operation can be applied to the separated upgoing waves in order to remove all existing multiples. The logic for designing the inverse filter operator for the upgoing waves on the basis of the downgoing waves for the zero-offset VSP data (called "up/down" or "up over down" deconvolution) is illustrated in Figure 12.9.

The IPP that enables the interpreter to determine the effect of the application of the inverse filter (up/down deconvolution) on their data is shown in Figure 12.10. Panel 1 (Fig. 12.10) shows the nondeconvolved upgoing waves (+TT) and panel 2 shows the effect of applying the median filter to the separated upgoing waves of Panel 1. Panel 3 (Fig. 12.10) shows the nondeconvolved up- and downgoing waves in -TT time. The separated upgoing waves are shown in panel 4 in -TT time. Panel 4 can be compared to the deconvolved upgoing waves in -TT time in panel 5. The comparison of panel 4 and 5 enables estimation of the effect that deconvolution has on the dataset. One of the results of applying a downgoing wave designed inverse filter to the upgoing waves is to change the polarity of the output dataset. Panel 5 (Fig. 12.10) is opposite polarity to panel 4. This polarity change is compensated for in the next two panels. The deconvolved upgoing data in panel 6 (+TT) is median filtered and shown in panel 7.

The interbed multiples are evident on an examination on panel 4 (Fig. 12.8). The multiple reflection generating strata lies at a depth of approximately 2160 m (Mannville Gp coal). The multiples reverberate and influence the seismic markers for about 200 to 300 ms beyond the recording of the interpreted coal bed event. These multiples have no significant effect on the primary zone of interest, the Leduc Fm at 2930 m.

INSIDE AND OUTSIDE CORRIDOR STACKS

Two types of IPP displays have been designed to enhance the recognition of multiples and the possible influence on interpretation of the surface generated and interbed multiples (Figs. 12.11, 12.12, 12.13) on the dataset. These are called the Inside and Outside

Figure 12.8. The interpretive processing panels that shows the wavefield separation operation in detail. The multiples and primary reflected waves can be traced from the raw data to the upgoing separated data.

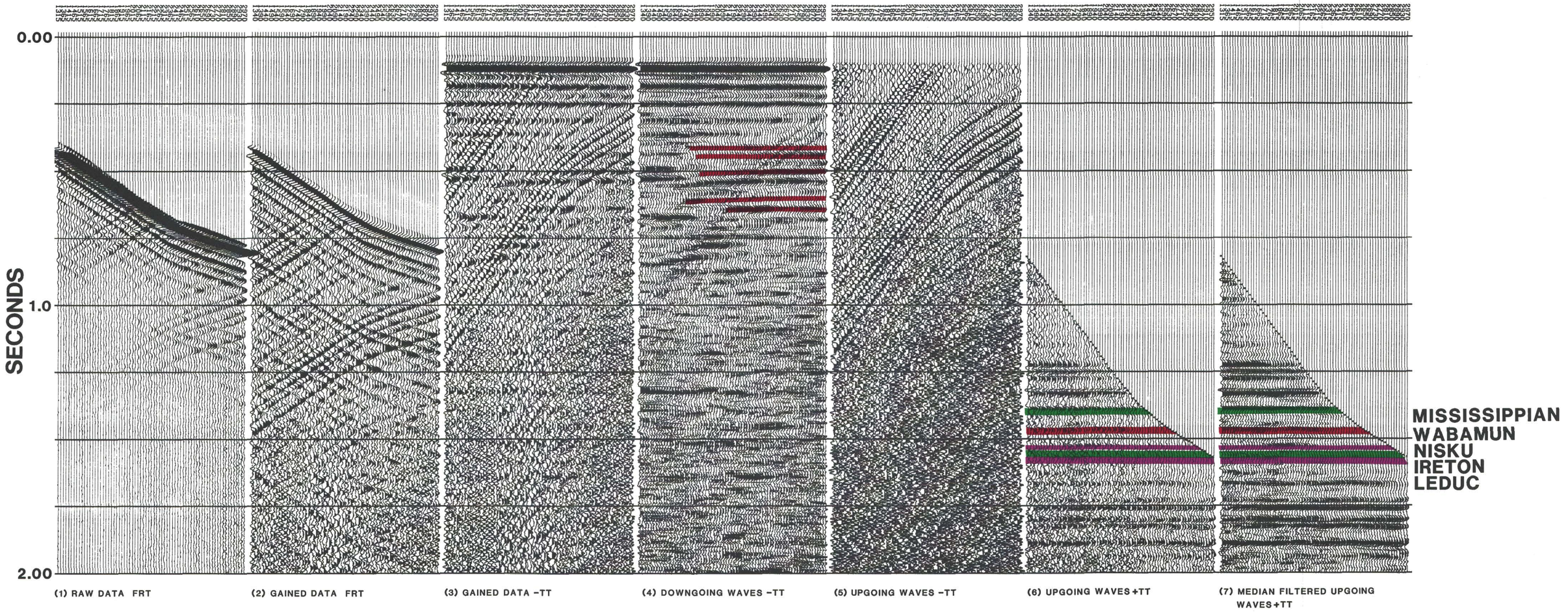

DONOR: GULF CANADA RESOURCES LIMITED | PROCESSOR: INVERSE THEORY AND APPLICATIONS, INC. | AUTHOR: R.C. HINDS

Figure 12.10. The interpretive processing panel that shows the effect on up/down deconvolution on the upgoing wave datasets. The separated downgoing waves display the downgoing primary and the downgoing multiples. The downgoing multiples are collapsed to the first break wavelet by deconvolution. The same operator is applied to the upgoing waves. The median filtered deconvolved and nondeconvolved upgoing waves in (+TT) time can be directly compared in order to estimate the reliability of the deconvolution operation for the zero-offset case.

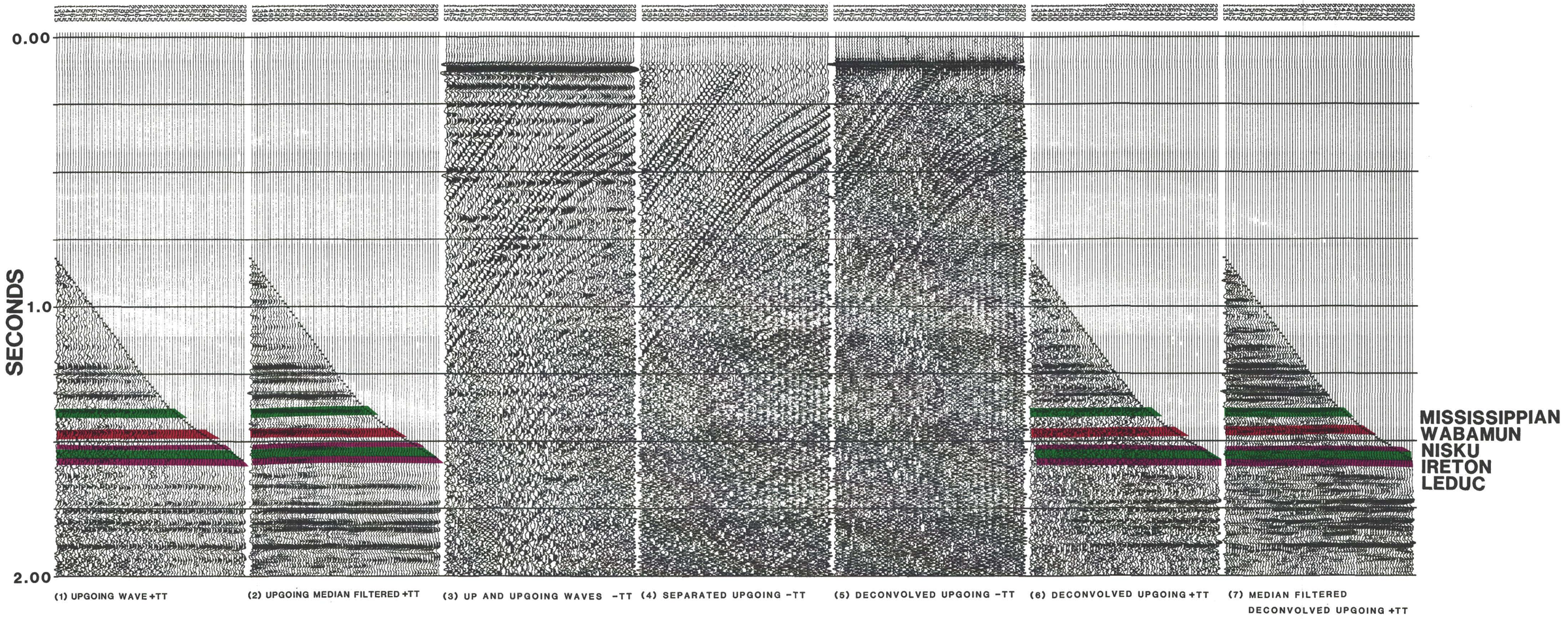

DONOR: GULF CANADA RESOURCES LTD. | PROCESSOR: INVERSE THEORY AND APPLICATIONS, INC. | AUTHOR: R.C. HINDS

Corridor stacks. The logic behind the displays is shown in Figure 12.11. At the Base of Fish Scales, Viking and Mannville reflectors, interbed multiples that affect the appearance of the Glauconite and Basal Quartz events are generated. The seismic signatures of the Cardium and the low velocity sequence around 1890 m depth also seem to be contaminated by multiples originating around 1740 m. In order to analyze the multiple pattern and interference, the geological tie with the VSP (to be presented below in the integrated interpretive display) and all of the corridor stacks plus the VSP panels upon which the corridor stacks were derived must be analyzed.

The interpretive processing panel display for the nondeconvolved outside corridor stacks positively bias the primary events and the nondeconvolved inside corridor stacks contain primary and multiple events (Fig. 12.12). Both the inside and outside corridor stacks of the deconvolved upgoing wave data should contain primary reflection events only (this panel is a test of the deconvolution operator) and are displayed in the IPP in Figure 12.13.

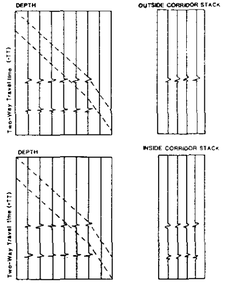

Figure 12.11. The logic for inside and outside corridor stacks of nondeconvolved zero-offset (VSP) data. The outside corridor stack contains the events in the narrow nonmuted corridor around the first break curve. The primary reflected upgoing waves intersect the first break curve so that a stack of these data will yield predominantly primary events. The inside corridor stack will contain both primary and multiply reflected upgoing waves. A comparison of the two stacks will indicate the possible multiple contamination in the VSP data. If the input data for the corridor stacks were deconvolved data, then the two stacks will be an indication of the reliability of the deconvolution operator. If the deconvolution is successful, then the inside and outside stacks of the deconvolved data will be approximately the same.

The interpretational differences in these corridor stacks can be due to:

1) the presence of multiples on the nondeconvolved inside stacks; and

2) the depletion of multiples on the outside nondeconvolved corridor stacks because the multiply reflected upgoing events do not intersect the first break curves;

The processing problems involved in the usage of these panels are:

1) the application of an inappropriate multiple deconvolution operator which could cause phase shifts and ringing. This also pertains to whether the operator was constructed from the downgoing waves using the concept that each trace will have an operator designed from that particular trace, from the top set of traces to positively bias the surface-generated multiples or from the last set of traces from the bottom of the borehole;

2) some processing systems having confusing gains and gain ramps built into the software to cosmetically upgrade the look of the data (the interpreter should investigate exactly how a processor's software handles the amplitude of the data);

3) the corridor chosen being too wide in order to alienate the short period interbed multiple; and

4) the wavefield separation technique and data enhancement method has added spurious events at the first breaks (the median filter can repeat traces at the first break curve which may represent noise that was generated by the wavefield separation operation).

In this regard, the inside corridor stack of the deconvolved data should look like the outside corridor stack. The interpretation of the amplitude differences on the corridor stacks should account for the fact that some of the rays of the events on the inside stacks have travelled through layers such as the Wabamun and Viking twice in order to reach the geophone whereas some of the reflections on the outside corridor stacks have only travelled through these layers once. This causes differential attenuation of the higher frequency data.

In the zones of interest, the deconvolved and nondeconvolved corridor stacks can be compared. Whether or not the zones suffer from multiple interference can then be determined. This can be further investigated on surface seismic data using closely spaced common offset panels.

The corridor stack panels consist of the non-muted input upgoing wave data, the muted corridor data and the resultant corridor stack. Comparison of the input data for the outside corridor stacks of the nondeconvolved and the deconvolved data in Figures 12.12 and 12.13 show that the input upgoing VSP data represents essentially flat lying events. One assumption in the usage of the corridor stacks is that the data image horizontal reflectors in the local area of the borehole. This can be confirmed by the observation that the VSP would be sampling at the most only 100 m from the bottom of the borehole with the shallowest receiver (by using a 200m offset) and that the data appears flat.

The panels are analyzed by examining the corridor of data that will be horizontally summed. The corridors may be contaminated by median filter artifacts created by the applied median filter encountering the first breaks. One should be convinced that the horizontal sum from the muted corridor data represents the input data. The two outside corridor stacks, nondeconvolved and deconvolved, differ slightly just below the Mannville event for approximately 200 ms and then match each other from the Pekisko event down to the bottom of the section. This means that the interbed multiple is of such a short period that the nondeconvolved outside corridor stack was unable to completely represent only primary reflections in that zone. This was point (3) in the discussion on the problems of the corridor stacks. The observation of most importance for the interpreter is that the Nisku and Leduc events do not seem to be influenced by the interbed multiple interference.

Comparison of the inside corridor stack of the deconvolved data and the outside corridor stacks of the deconvolved and nondeconvolved data show that the up/down deconvolution has successfully removed the Mannville/Basal Quartz interbed multiple in the data of the inside corridor. The peak for the reflector between the Mannville and the Basal Quartz has been preserved on all of the traces of the deconvolved data. In order to estimate the multiple content of the data, the nondeconvolved inside and outside corridor stacks can be compared. Once again, the Mannville interbed multiple shows up as the main disturbance in the data. Fortunately, the multiples can be removed by the up/down deconvolution of the data.

Other methods create transposed corridor stacks that take into account slightly dipping interfaces about the borehole and the interpretation pitfalls associated with the usage of that resultant data will be discussed in later research.

THE INTEGRATION OF OTHER INTERPRETATION DATA

The Integrated Interpretive Display (IID) is one of the first views of the VSP data merged with the entire suite of exploration information such as well log and surface seismic data. Modified versions of this display could contain other seismic lines in the area. As shown previously, the IPP allows the interpreter to gain confidence in the processing steps. Both types of presentations are necessary to ensure that a complete set of displays are available to the exploration team in order to enable full exploitation of the subsurface images found in the VSP or LSP data.

The interpretation of the IID typically begins with the sonic and gamma logs displayed in depth. Other logs to indicate porosity and electrical character can also be plotted on the display. Well-logs in true vertical depth can be used for slightly deviated boreholes as long as the VSP, placed directly beneath the well logs, is plotted with the same depth scale. The VSP traces should be plotted relative to absolute depth so that the geophone traces are spaced accordingly. As an example, the Wabamun in the VSP well was interpreted to be at a depth of 2616 m whereas the nearest depth trace for the VSP is at 2610 m. The sonic log and gamma-ray log response of the Wabamun Gp are shown in Figure 12.14 as a sharp decrease in the gamma-ray reading and as an increase in velocity in the sonic log at the 2616 m level. The vertical depth location can be followed down the VSP trace to the first break located around 1450 ms on the 2610 m geophone depth trace. Visually interpolating between the 2610 m trace and the next deeper trace allows one to interpret the primary Wabamun seismic event.

Figure 12.14 illustrates that the main seismic markers can be interpreted on the VSP using this method. The seismic markers having been tied to the geological depths are now represented in two-way traveltime, the common bond between the surface seismic and the VSP in +TT time. The interpretation can be followed to the left to the well location on the surface seismic and onto the inside and outside corridor stacks. Away from the well location the seismic markers can be interpreted noting that the Glauconite to Banff sequence and the top of the Leduc are poorly represented on the surface seismic data. The seismic signatures of Glauconite to Banff units suffers slightly from destructive interference. The top of the Leduc reef was interpreted before the drilling of the well to be the

Figure 12.12. The inside and outside corridor stacks of the nondeconvolved data for the zero-offset Lanaway/Garrington VSP. The corridor stacks are presented altogether on the same interpretive processing panel to allow for an analysis of the multiple contamination of the data. The input data in both polarities along with the displaying of the muting zones indicate the reliability of the stacks as a representation of the main seismic events and corresponding multiples in the data.

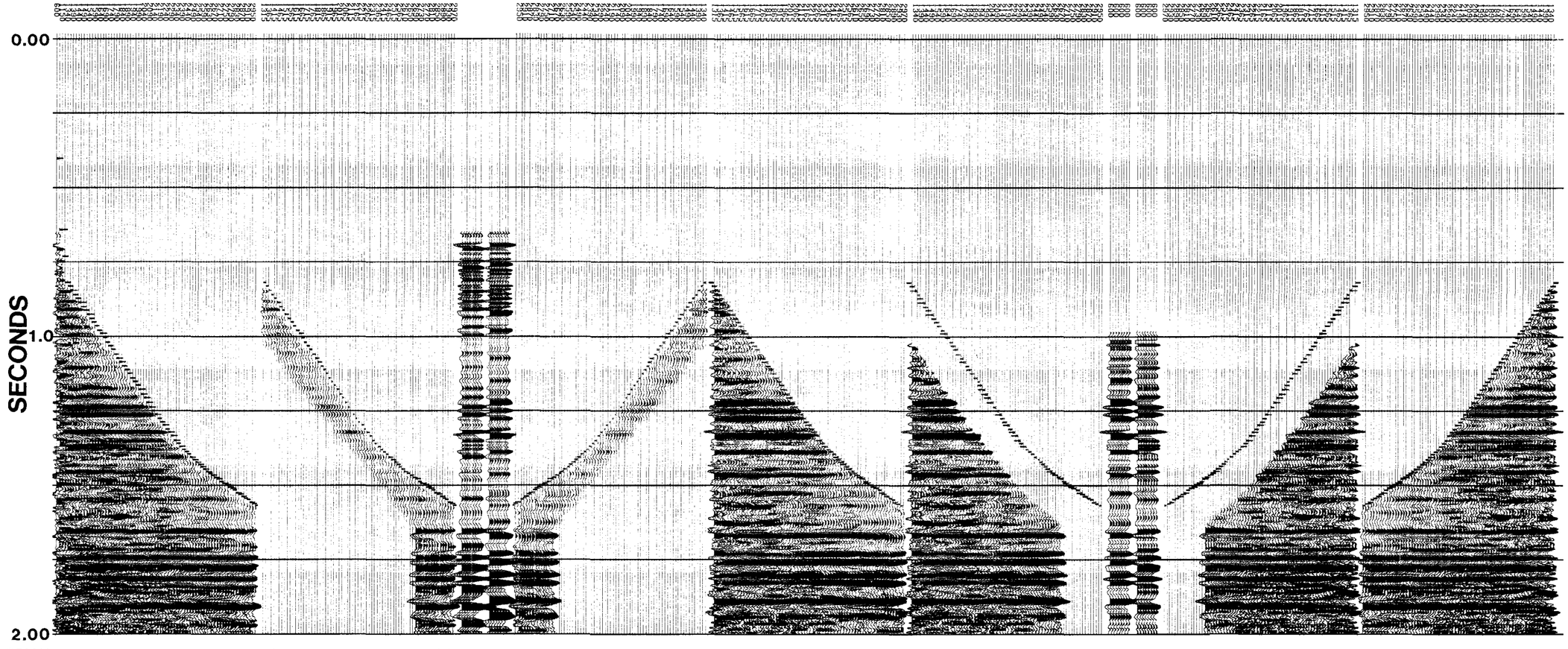

DONOR: GULF CANADA RESOURCES LTD. | PROCESSOR: INVERSE THEORY AND APPLICATIONS, INC. | AUTHOR: R.C. HINDS

Figure 12.13. The inside and outside corridor stacks of the deconvolved data for the zero-offset Lanaway/Garrington VSP. Both of the corridor stacks should approximate the primary upgoing wave events with the minimal contamination of upgoing multiples. This panel can be used to analyze the reliability of the deconvolution operation.

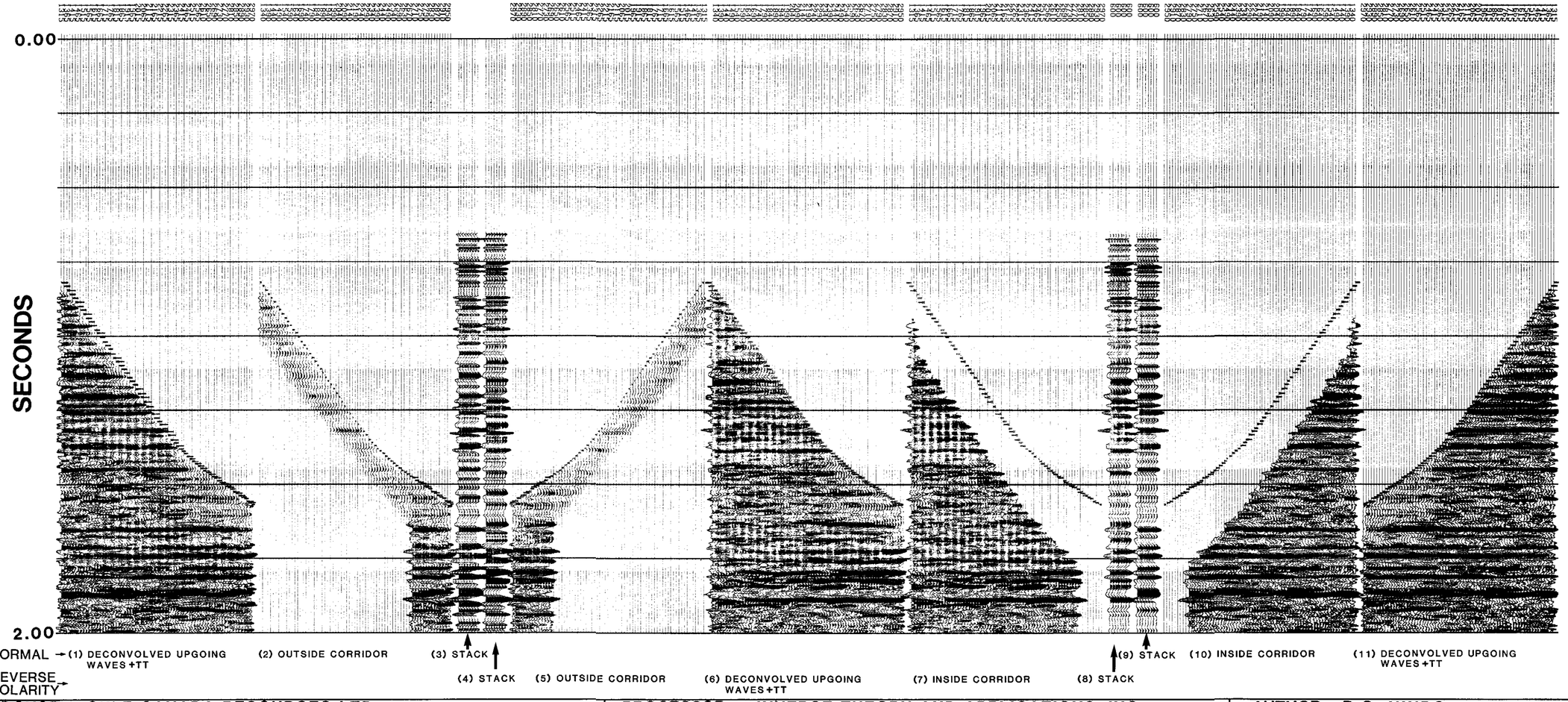

DONOR: GULF CANADA RESOURCES LTD. | PROCESSOR: INVERSE THEORY AND APPLICATIONS, INC. | AUTHOR: R.C. HINDS

Figure 12.14. The integrated interpretation display for the zero-offset Lanaway/Garrington well. The interpretation of the panel begins with the tie of the VSP depth axis with the depth axis of the sonic and gamma-ray logs. The interpreted geologic events are tied to the VSP at the first break curve of the VSP. Choosing the Wabamun Gp marker at 2616 m, one locates the depth trace of the VSP for that log depth and the primary upgoing event that intersects the first break time of that trace should be the VSP Wabamun Gp event. The surface seismic, synthetic seismogram and corridor stacks are tied to the (+TT) time of the VSP. For a comparison of the tie of the primary event (outside) corridor stack and the synthetic seismogram to the well log data, the sonic and gamma ray logs are plotted in time.

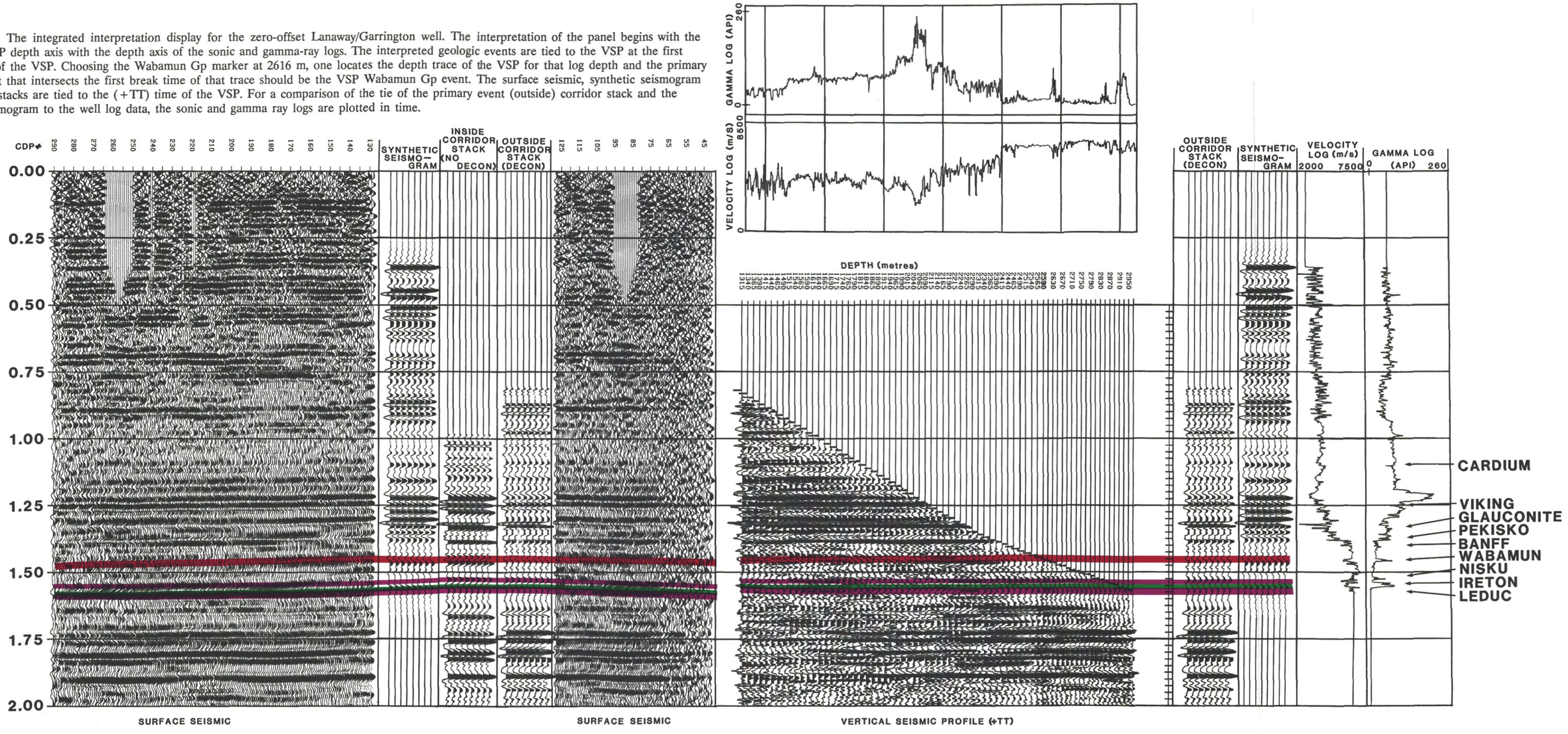

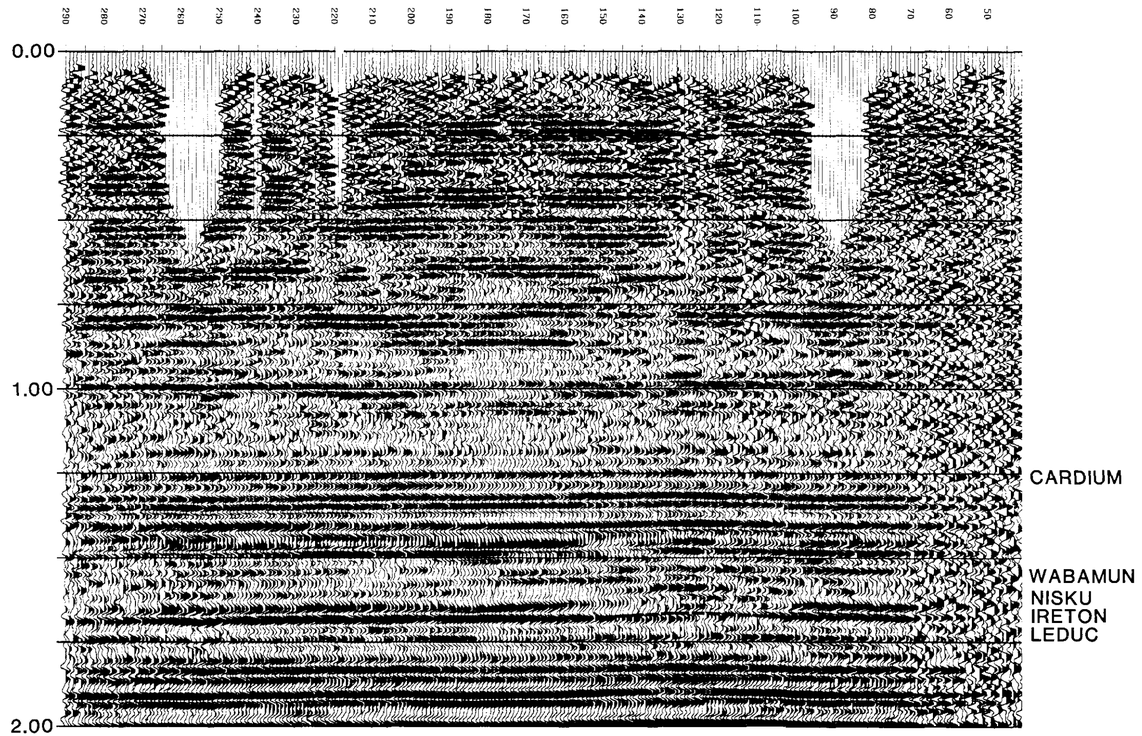

Figure 12.15. The reinterpreted surface seismic section incorporating the VSP interpretation. The previously interpreted reef top at the well is 12 ms above the VSP interpreted Leduc reef top. This accounts for the 20-30 m loss of expected reef build-up and both the VSP and reinterpreted seismic section tie the isopach values from the well logs.

peak overlying the regional Leduc event. The VSP corridor stacks show that the trough above the regional Leduc event is the location, in time, of the structurally higher Leduc anomaly. The surface seismic did not image the flexure of the reef properly at this location.

The inside and outside corridor stacks, plus the synthetic seismogram imposed between the two separate parts of seismic section (separated at the well location), allows comparison of the multiple contamination and evaluation of the synthetic seismogram to indicate the zone of interest. The corridor stacks show minimal multiple contamination around the zone of interest, the Leduc Fm. The synthetic seismogram poorly represents the Nisku to Ireton sequence. A possible explanation for the sonic misrepresentation may be revealed in the observation that the fluid (mud) in the borehole was increased in density to safeguard against destabilization of the fluid column by any highly-pressurized fluids from porous zones around the borehole. This causes a mud-cake in the porous Leduc Fm which may affect the sonic log readings enough to cause the synthetic seismogram to poorly represent the true acoustic impedance.

To the right of the VSP (Fig. 12.14) is the outside corridor stack (containing predominantly primary events), the synthetic seismogram and the two well logs converted to time. This allows an evaluation of the reliability of the corridor stack and synthetic seismogram. Because the synthetic seismogram is calculated from the finely depth sampled sonic log, in some areas the synthetic will have higher resolution than the corridor stack. Since the range of the wavelengths contained in the VSP are the same as for surface seismic, in some zones the corridor stack will tie to the seismic better. Thus, the corridor stack does not need to be stretched to fit the clastics part of the seismic section and then restretched to fit the carbonate part of the seismic section.

The interpretation of the IID has allowed the creation of an exploration picture around the well location and the investigation of the seismic signature of the top of the reef at the borehole. The interpretation performed on all of the interpretive displays lead to a reinterpreted post-VSP surface seismic section shown in Figure 12.15. Other look-alike anomalies on seismic lines in the area may also be economically productive as was this case history well, therefore justifying the use of this technique.

LATERAL SEISMIC PROFILE (LSP) CASE HISTORY

REGIONAL GEOLOGY AND GEOPHYSICS

The Lateral, or Multi-offset, Seismic Profile (LSP) example is from the Ricinus field which is located approximately in Twp 34 Rge 8 W5M (Fig. 12.2). The oil and gas production from the Ricinus field is from 40 separate Cardium pools, four Viking pools, two Leduc (D-3) pools and unassigned pools. The target of the VSP well was the D-3B pool which to date has produced 5,645,093 MCF of gas along with 16,912 BBL of water as of September 1987. The areal extent of the D-3B pool can be estimated to be 25-30 mi^2. In the separate D-3A pool (from the Leduc atoll to the northwest), 71,113,835 MCF of gas and 286,371 BBL of water have been produced from three producing wells as of September 1987.

The primary target of the VSP was the updip edge of the gas prone Leduc Fm atoll. Three wells are shown in the geological cross-section shown in Figure 12.16. The well that was used for the VSP will be referred to as the "VSP well". The other two wells will be referred to as "well A" and "well B". Well A in the geological profile penetrated approximately 400 m of Leduc reef whereas well B located updip in the same pool encountered a thicker gas zone than the shut-in potential gas well A. As shown in the geological section the geological markers above the reef are the Elkton Member of the Turner Valley Fm (limy dolomite), Shunda Fm (limy dolomite), Pekisko Fm (limy dolomite) and Banff Fm of the Rundle Gp (limestone), the Wabamun Gp (anhydritic dolomite and anhydrite), the Nisku Fm (dolomite) and the Ireton Fm (shale). Off-reef formations include the Ireton Fm, the Westerdale marker (shaly limestone), and the Duvernay Fm (shaly dolomite). Underlying the Leduc reef are the Cooking Lake Fm (dolomitic limestone), and the Swan Hills Fm (dolomite) which unconformably overlies the Elk Point Gp. Interpreted on the seismic section is a near-Cambrian marker.

The surface seismic line with the pre-drilling interpretation is shown in Figure 12.17. One kilometre to the west of the VSP well location, the surface seismic displays drape at the Wabamun Gp level and pull-up of the near-Cambrian event under the interpreted Leduc reef. The well was drilled with the expectation that the updip edge of the atoll would be intersected. The Mesozoic faulting in the area complicates the interpretation of the surface seismic by causing

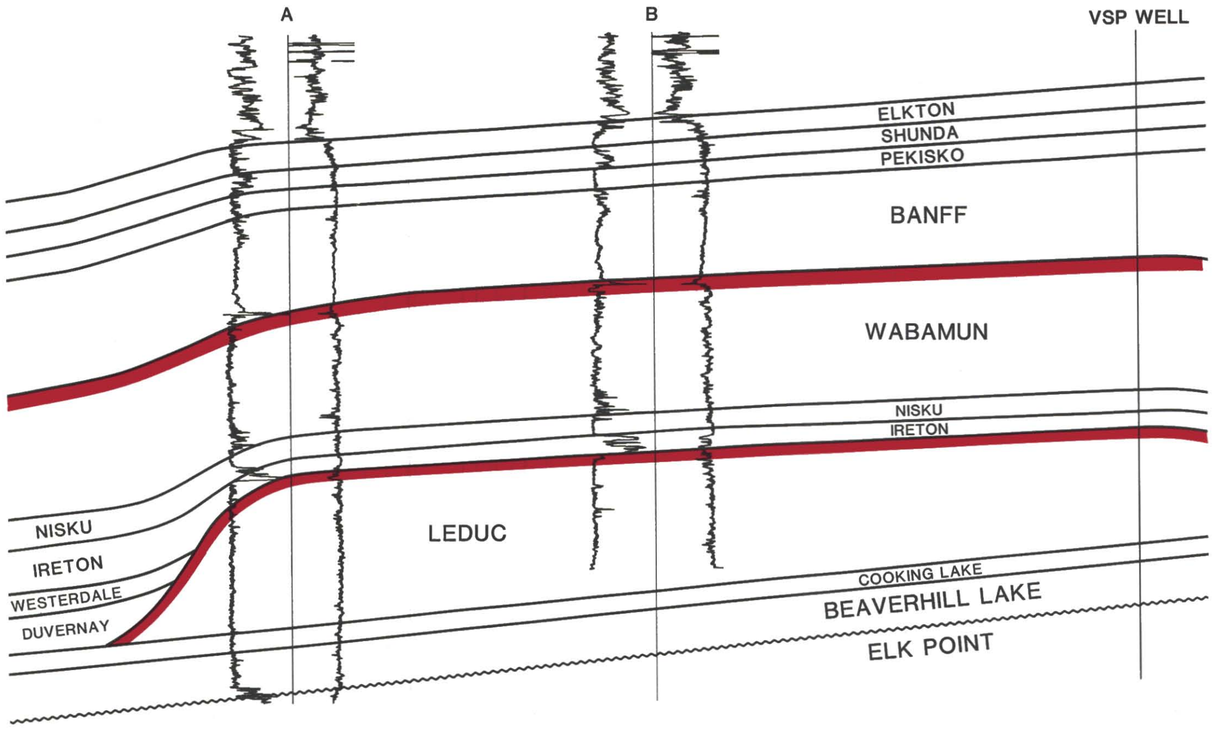

Figure 12.16. The predrilling geological section for the D-3B Ricinus pool. The main markers in the section are the Elkton, Shunda, Pekisko and Banff Units of the Rundle Gp (Mississippian), the Wabamun Gp, the Nisku Fm, the Westerdale Limestone unit (sometimes called the "fast Ireton"), the Duvernay Fm, the Leduc Fm atoll, the Cooking Lake Fm, the Swan Hills Fm and the Elk Point Gp. Well A was drilled on the downdip side of the reef and encountered less gas reserves than did Well B which is located updip. The predrilling prognosis for the VSP well was that the well would be updip and still be above the gas/water contact.

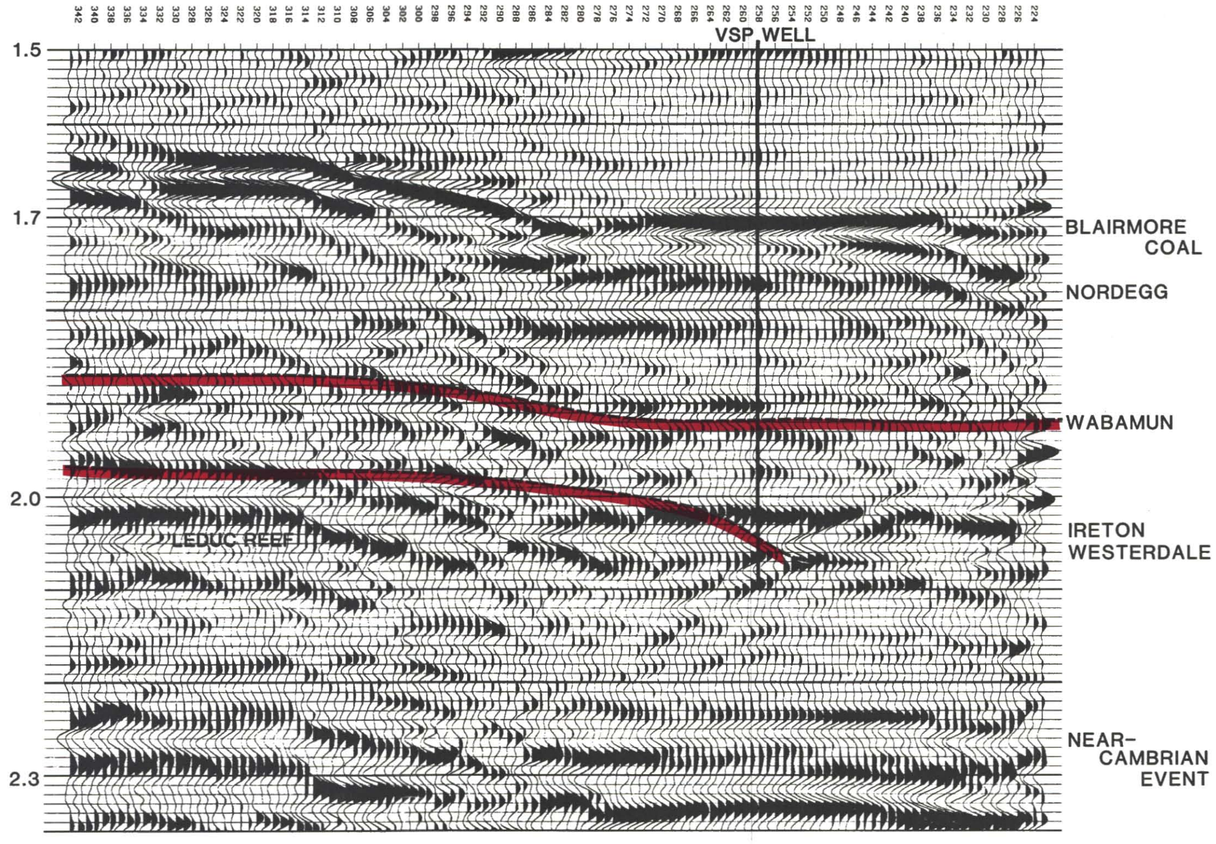

Figure 12.17. The predrilling surface seismic line. The upper section of the line is distorted due to faulting in the Mesozoic section. At the VSP well location, the Ireton Fm is interpreted to rise onto the reef. The Wabamun shows drape from reef to off-reef of approximately 10 ms. The near Cambrian event (trough) displays about 5-10 ms of pull-up under the interpreted reef. This amount is decreased from normal pull-up for Leduc reefs because the off-reef section around the reef does not consist entirely of low velocity shales but also is made up of the Westerdale Limestone (which is about the same velocity as the reef). The labelled main seismic events in this figure are the Nordegg Fm, Ireton Fm, Leduc Fm, Westerdale Unit, Duvernay Fm, Cooking Lake Fm (from the VSP interpretation) and a postulated near-Cambrian event.

confusing time structural anomalies in the data at the Viking Fm level down to the near-Cambrian event.

A thick off-reef Ireton, Westerdale limestone and Duvernay Fm were encountered in the VSP well. The VSP/LSP survey was run in order to:

1) establish an accurate seismic tie with the geology in the area;

2) determine the effect of multiple interference on the seismic (and VSP) dataset; and

3) determine whether the edge of the Leduc Fm reef can be interpreted to be in the near vicinity of the well (between 0 and 500 m).

Two offsets were used in the survey, at 200 m and 1100 m, in the direction of the interpreted Leduc reef. The interpretation of the "zero-offset" Interpretive Processing Panels (IPP) will be presented below without the lengthy technical explanations already done in the Lanaway/Garrington VSP example.

ZERO-OFFSET VSP

At a distance of 200 m away from the well, the source is still considered to be at a zero-offset location. The drilling rig was placed on a prepared area called the wellpad which was 2-3 m above the ground level. The wellpad was 100 by 100 m and constructed of trucked-in sand and mud. The VSP energy source was placed down from the well lease pad and amongst trees in order to minimize any possible tube wave problem. The presence of the trees, roots and the change of elevation aided in the destructive interference of the tube wave. The surface source was Vibroseis and the triaxial sonde depth spacing was 30 m from a depth of 4350 m up to 420 m. Above 420 m, the depth spacing was 60 m up to the shallowest level of 180 m. Several records were obtained as the sonde was lowered down the borehole and these station locations were repeated during the production run from the bottom to the top of the borehole. These uphole data served as quality control traces used to detect any possible cable stretch or cable depth counter malfunction. These traces aided in the setting of the gain amplifiers on the recording instruments before the production VSP begins at the bottom of the borehole.

A wall-locking geophone sonde with a triaxial geophone assembly was used in the borehole. As the tool is pulled up the borehole and locked into place at designated depth interval, the sonde will change direction orientation in the borehole. For the non-zero offset data, the orientation of the two horizontal and single vertical geophone in the borehole will be referenced using an orthogonal coordinate system. Hodogram analysis will be used. Such an orthogonal coordinate system is shown in Figure 12.18. At each geophone location, the local geophone axis will be referred to as X,Y and Z (also shown in Figure 12.5 for the deviated borehole). For the zero-offset data, only the Z axis geophone data is considered (similar to the data analysis in the Lanaway VSP example).

As an additional note, for mineral exploration situations where the object may be to show the areal extent of a steeply dipping reflector, the zero-offset VSP data interpretation can make use of all three geophone components. For this case, the hodogram analysis for the far-offset LSP is used to rotate such zero-offset data if the two offsets were acquired during the same production run in the borehole.

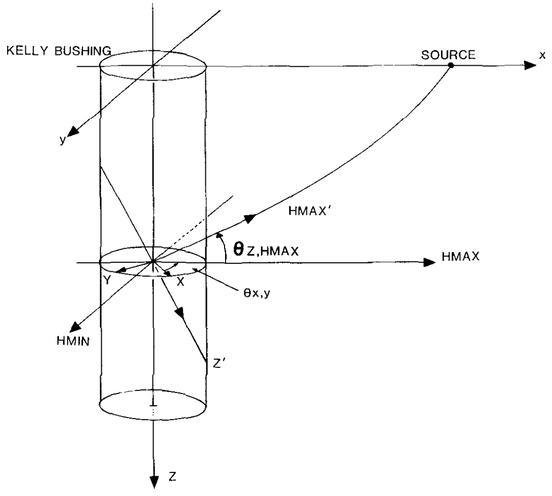

Figure 12.18. The orthogonal coordinate system of the local X, Y and Z geophone along with the coordinate axis that will be used as the principal axis in hodogram analysis.

WAVEFIELD SEPARATION

The IPP which illustrates the processing from raw data stage to the wavefield separation stage is shown in Figure 12.19. The data when aligned along the first breaks (–TT) in panel 3 show surface generated downgoing multiples (appearing as horizontal events after the first wavelet down to 400-500 ms). Comparing the gained data in FRT (field recorded traveltime, panel 2), the interpreted near-Cambrian reflector can be followed up to its representation on the traces for the shallowest geophone location (recorded on the shallow depth location geophone around 2200 ms FRT). Looking at the gained data, the upgoing near-Cambrian event turns into a downgoing multiple and begins to travel downwards. This Cambrian-to-surface downgoing multiple is displayed on the downgoing aligned data in panel 3 as the series of events around 2000 ms. This example of tracing multiples from the raw data panel onto the downgoing wave panel can be done for most of the visible multiples.

The strongest events on the separated upgoing wavefield panel after the data is placed into (+TT) time (pseudo two-way traveltime) are the Viking Fm, Nordegg Fm, Wabamun Gp, Ireton Fm, Westerdale limestone, Duvernay Fm and the postulated near-Cambrian event.

DECONVOLUTION

The downgoing-aligned waves (panel 3 shifted into –TT time in Fig. 12.19) showed that the data was affected by surface-generated downgoing multiple contamination. The VSP deconvolution process is illustrated in Figure 12.20. The deconvolved data can now be used in the corridor stack analysis panels in order to determine the extent of the effect of the multiples on the data.

INSIDE AND OUTSIDE CORRIDOR STACKS FOR MULTIPLE RECOGNITION

The inside and outside corridor stacks of both the nondeconvolved and deconvolved zero-offset data are displayed in Figures 12.21 and 12.22, respectively. The multiples in Figure 12.21 are coded and when compared with the multiple attenuated outside corridor stack (of the nondeconvolved data) the surface and interbed generated multiples are seen to extend throughout the entire VSP section.

The Viking, Ireton, Westerdale and Duvernay formation events, however, are relatively unaffected by the multiple wavetrain. The Wabamun Gp event, however, is severely affected by multiple interference. The nondeconvolved median filtered data displayed in (+TT) time in Figure 12.21 shows that the Wabamun Gp event is unaffected by multiple contamination (destructive or constructive interference) as the event intersects the first break curve. At that point the multiple which seems to originate from the Viking Fm or Nordegg Fm does not affect the primary upgoing wave from the Wabamun Gp. That multiple will exist on the VSP as an upgoing wave from the shallowest geophone location down to the trace of the bottom layer where the interbed multiple is generated (Figure 12.4b). On the VSP upgoing wave section, the Nordegg Fm multiple terminates beneath the point where the Nordegg Fm intersects the first break curve (+TT). The Wabamun Gp upgoing primary event will be unaffected at geophone locations beneath that depth level.

The deconvolved corridor stacks (Figure 12.22) show that the Wabamun Gp primary is a flat lying continuous event across the section once the effect of the multiple is minimized. At this point the surface seismic can be reinterpreted at the well location.

NON-ZERO OFFSET (LATERAL SEISMIC PROFILE)

In the zero-offset example, the wavefield separation technique attenuated the upgoing waves from the data using median filters. The underlying assumption was that the vertical geophone would record predominately P-wave energy and that the horizontal geophones recorded solely SH and SV energy. The amount of shear wave energy recorded by the horizontal geophones in the zero-offset geometry is assumed to be negligible. For the non-zero offset data, the downgoing and upgoing P-waves are partitioned onto all three geophone channels.

HODOGRAM ANALYSIS

Figures 12.18 and 12.23 illustrates that the data from the X,Y and Z channels can be rotated into a new coordinate system which, by assumption, should contain separated wavefield components (SH on one channel, Downgoing P and Upgoing SV on another channel and Upgoing P and Downgoing SV on the third channel). The method that is used to separate the X,Y and Z data into P,SH and SV components using windowed downgoing P wave first break data is called the Hodogram or Polarization Analysis (Hardage, 1983). Assumptions made in doing the hodogram analysis are:

Figure 12.19. The Interpretive Processing Panels for the zero-offset Ricinus VSP which shows the wavefield separation operation in detail. The multiples and primary reflected waves can be traced from the raw data to the upgoing separated data.

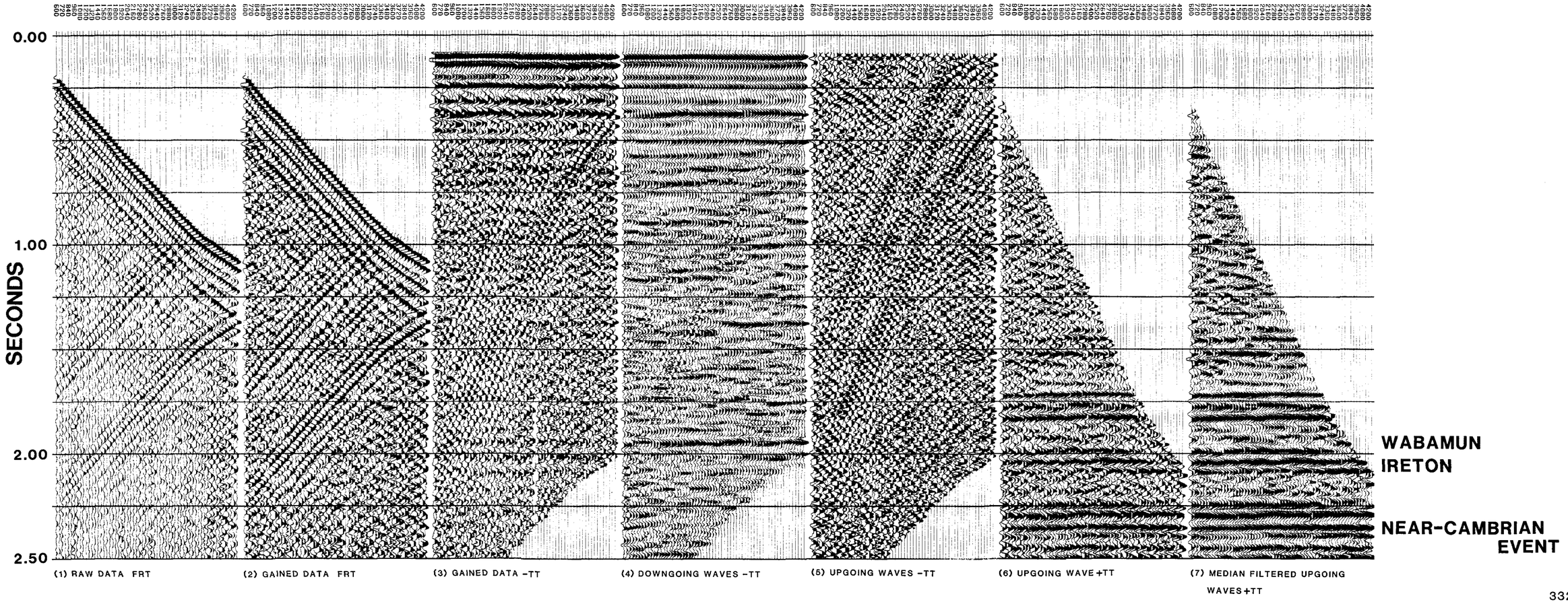

DONOR: GULF CANADA RESOURCES LTD. | PROCESSOR: INVERSE THEORY AND APPLICATIONS, INC. | AUTHOR: R.C. HINDS

Figure 12.20. The Interpretive Processing Panel for the zero-offset Ricinus VSP which shows the effect on up/down deconvolution on the upgoing wave datasets. The separated downgoing waves display the downgoing primary and the downgoing multiples. The downgoing multiples are collapsed to the first break wavelet by deconvolution. The same operator is applied to the upgoing waves. The median filtered deconvolved and nondeconvolved upgoing waves in (+TT) time can be directly compared in order to estimate the reliability of the deconvolution operation for the zero-offset case.

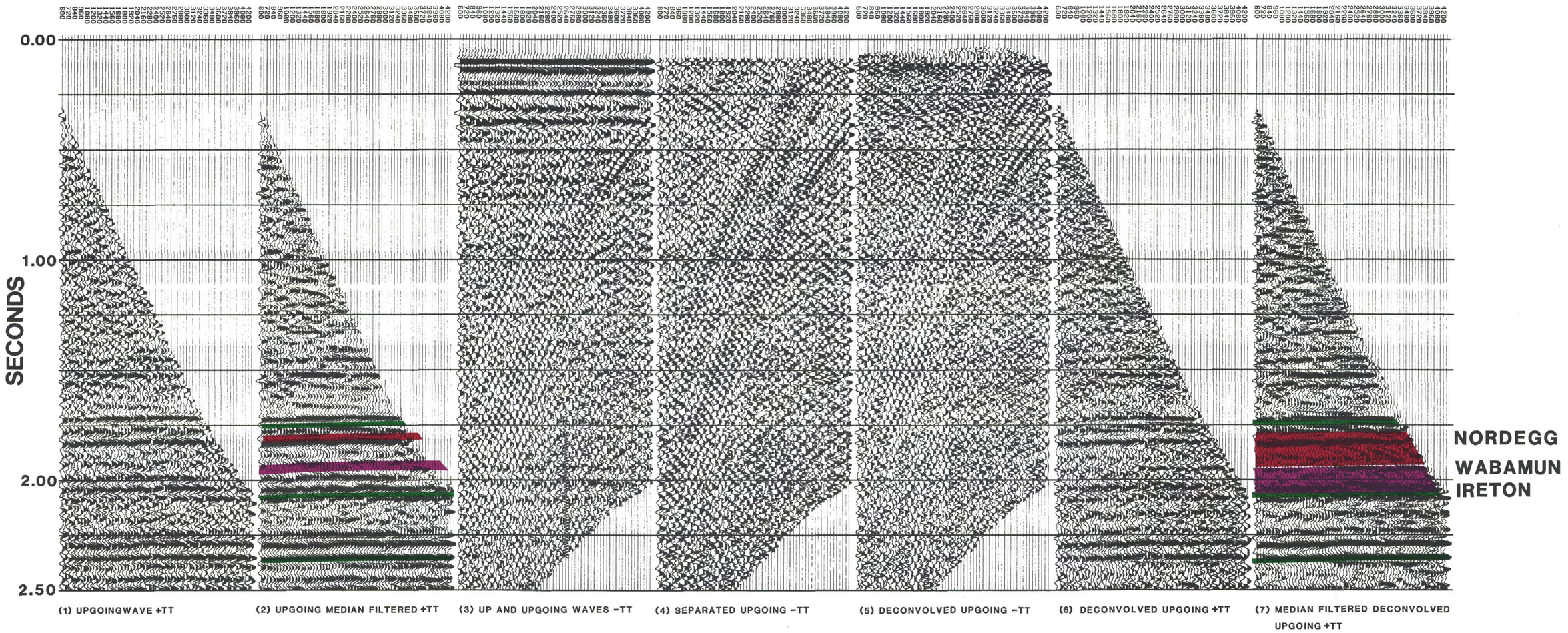

DONOR: GULF CANADA RESOURCES LTD. | PROCESSOR: INVERSE THEORY AND APPLICATIONS, INC. | AUTHOR: R.C. HINDS

Figure 12.21. The Inside and Outside Corridor stacks of the nondeconvolved data for the zero-offset Ricinus VSP. The corridor stacks are presented altogether on the same interpretive processing panel to allow for an analysis of the multiple contamination of the data. The input data in both polarities along with the displaying of the muting zones indicate the reliability of the stacks as a representation of the main seismic events and corresponding multiples in the data.

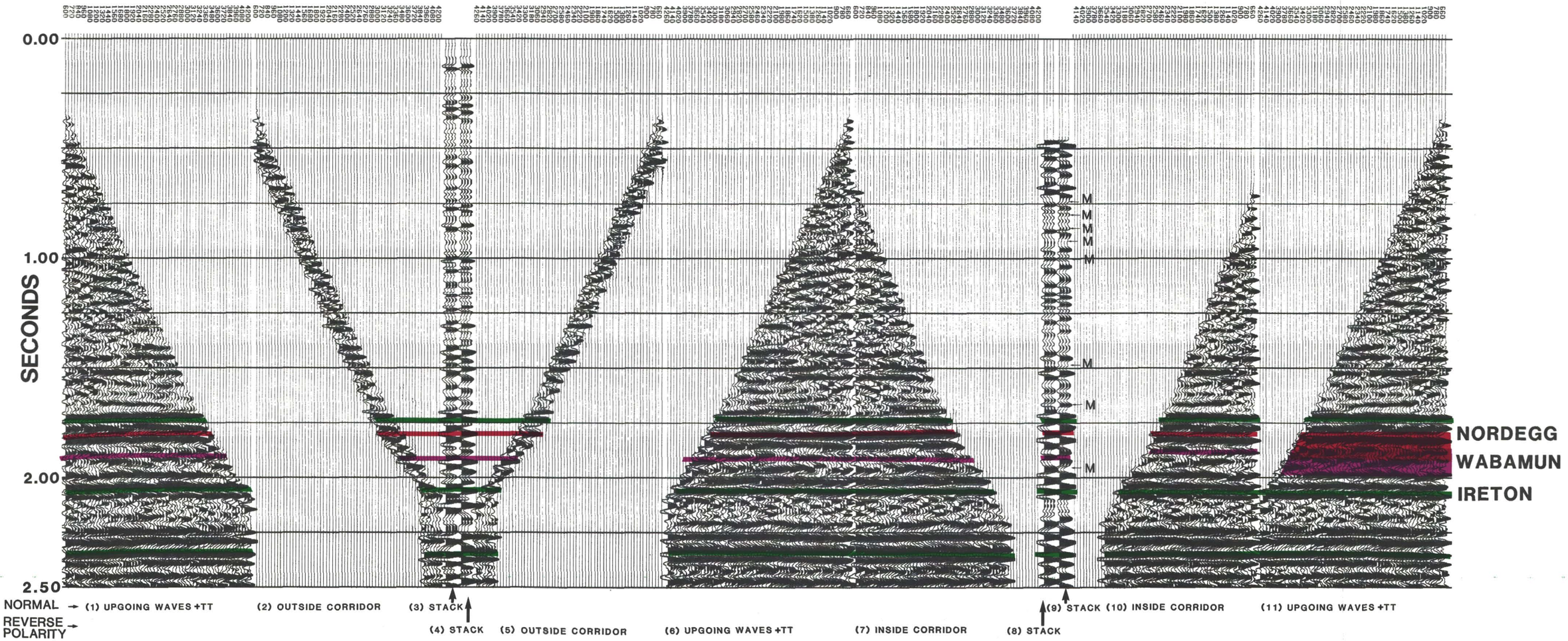

DONOR: GULF CANADA RESOURCES LTD. | PROCESSOR: INVERSE THEORY AND APPLICATIONS, INC. | AUTHOR: R.C. HINDS

Figure 12.22. The Inside and Outside Corridor stacks of the deconvolved data for the zero-offset Ricinus VSP. Both of the corridor stacks should approximate the primary upgoing wave events with the minimal contamination of upgoing multiples. This panel can be used to analyze the reliability of the deconvolution operation.

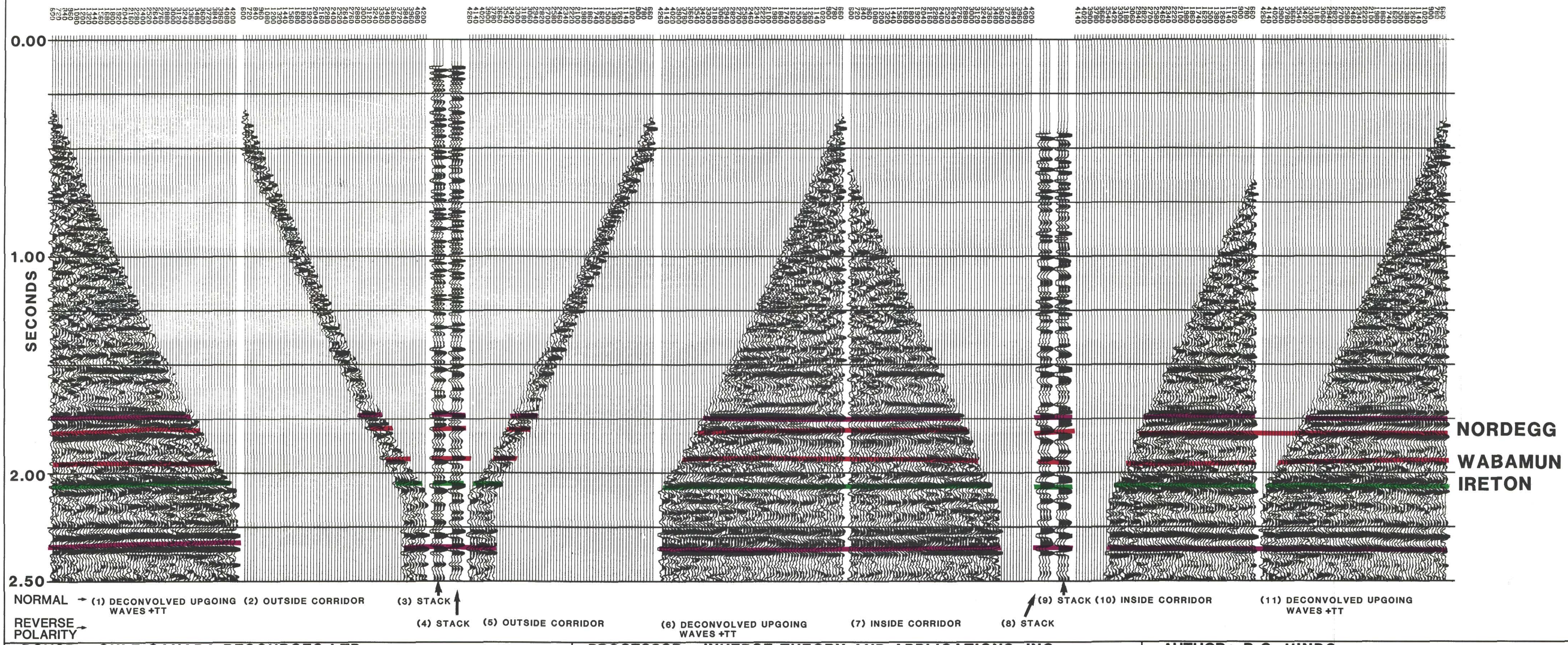

DONOR: GULF CANADA RESOURCES LTD. | PROCESSOR: INVERSE THEORY AND APPLICATIONS, INC. | AUTHOR: R.C. HINDS

1) P and SV downgoing and upgoing wave energy travel in the two-dimensional plane made by the borehole and the source;

2) the borehole is assumed to be vertical and in the plane of the source and the well;

3) the downgoing and upgoing waves arrive at right angles to each other at the geophone (Fig. 12.18 and 12.23);

4) the downgoing primary P-wave travels in the source-well vertical plane in an analysis window of one period (the source wavelet can be fully described by looking at one period of the primary P-wave after the first break arrival time); and

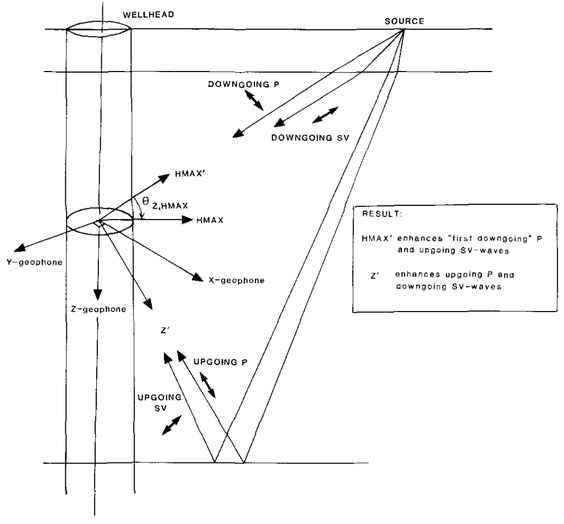

Figure 12.23. The orthogonal rotation axis used in the hodogram analysis. The geophone principal axis labelled Z' will contain mostly upgoing P-wave upgoing and S-wave downgoing energy. The geophone principal axis HMAX' will contain mostly P-wave downgoing and S-wave upgoing wave energy.

5) noise as a result of poor tool coupling and casing ring does not exist or is negligible on the data.

The initial stage of the polarization analysis is to rotate the X and Y geophone data numerically so that the resultant output channels have the P and SV downgoing energy maximized (HMAX) and the other channel has the P and SV downgoing energy minimized (HMIN). The method of numerically rotating the traces can be thought of as redistributing the amplitudes of the two input traces onto the two output traces. Taking the X and Y data at one geophone location, a hodogram is generated by plotting the respective amplitudes of the X and Y channel for each time sample over a given time window on the two traces. For the analysis of the P downgoing energy, the time window is a window around the P

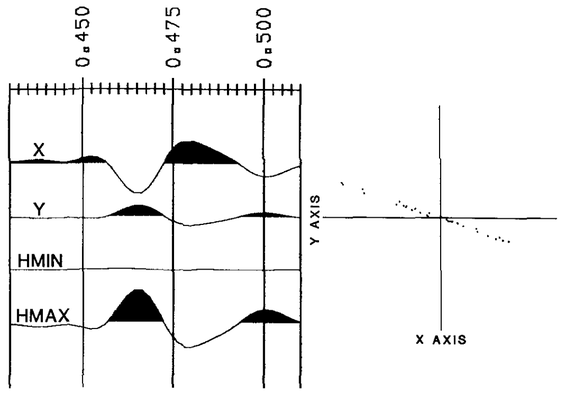

Figure 12.24. Hodogram analysis using the first break downgoing P-wave energy of the X and Y channels to rotate into the HMIN and the HMAX output channels. Windows are placed around the primary downgoing wave on the two input channels, X and Y. The respective amplitude values in the two windows are plotted onto a X, Y axis forming a hodogram. The angle that is traced by the hodogram is used in a two-by-two matrix for application on the two input channels in producing the two output channels. Ideally, this analysis should be done interactively at a computer terminal.

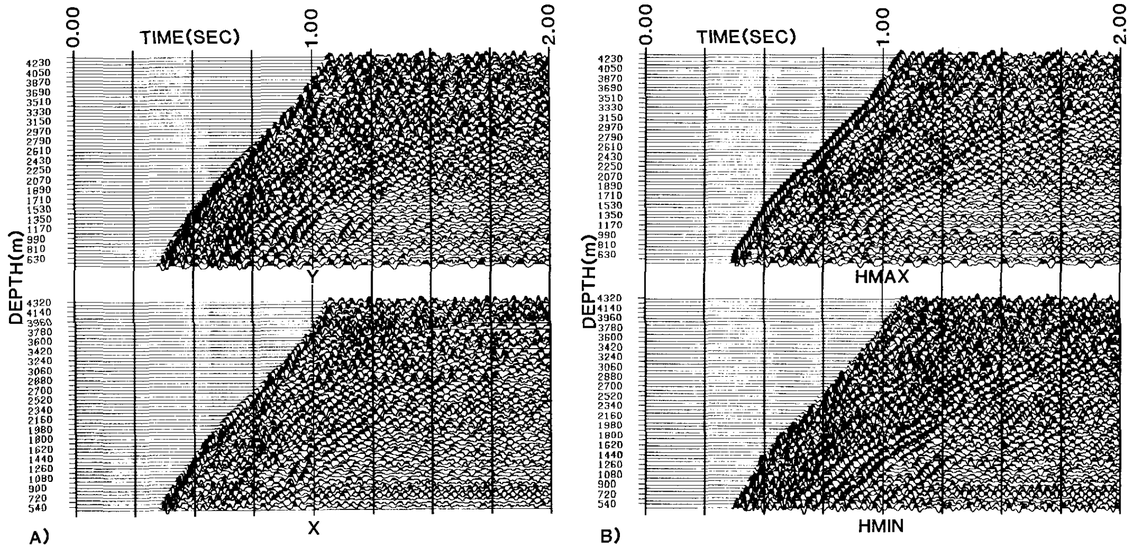

Figure 12.25. The result of the hodogram analysis for the X and Y channels on the Ricinus far-offset data. The X and Y channels are plotted along with the resultant HMIN and HMAX output datasets.

wave first break arrival on the two traces (Figure 12.24). The resultant data points will trace a curve called the hodogram of the particle trajectory. The angle that the curve makes with the coordinate system is used to numerically rotate the X and Y channels into the HMIN and HMAX channels (Fig. 12.18). This analysis should be done interactively by the recently developed interactive processing workstations.

The HMIN channel should contain minimal P and SV data being predominately SH energy (and out-of-the-plane reflections).

The inputs and outputs of the hodogram analysis where the X and Y channels have been transformed into the HMIN and HMAX

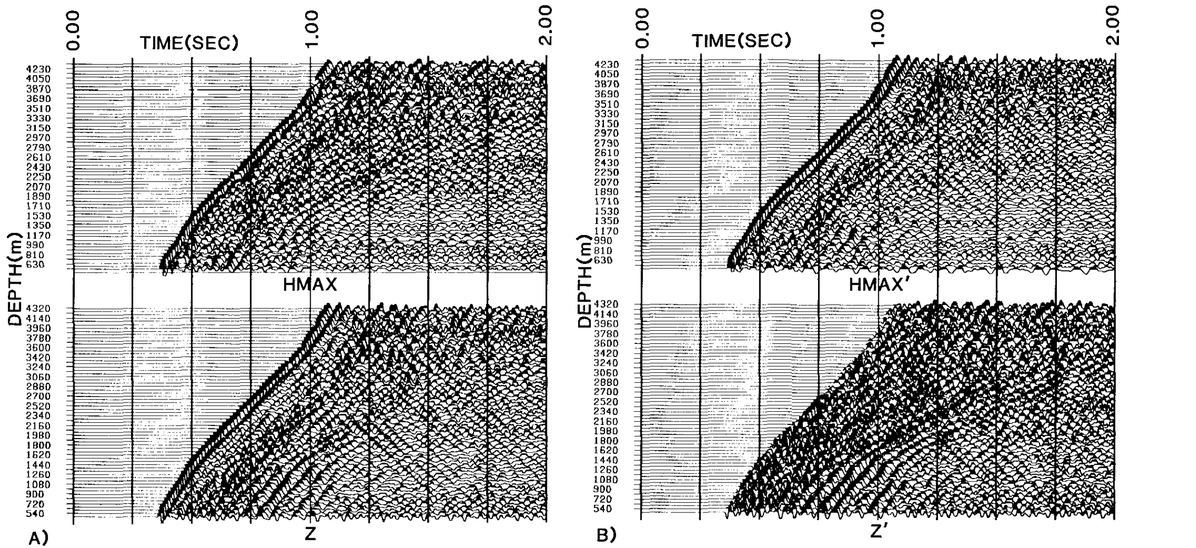

Figure 12.26. The result of the hodogram analysis for the HMAX and the Z channels on the Ricinus far-offset data. The Z and HMAX channels are plotted along with the resultant Z' and HMAX' output

channels are shown in Figure 12.25. The resultant HMIN channel should contain predominantly SH wave energy and P or SV energy that did not fit the assumptions of the analysis. Noisy data will be amplified and spread onto both of the resultant channels.

datasets. The HMAX' channel should contain mostly downgoing P-wave and upgoing SV-wave data. The Z' channel should contain mostly downgoing SV-wave and upgoing P-wave data.

The next rotation using the P downgoing waves takes a time window around the P wave first break curve on the HMAX and Z channel and the resultant hodogram rotation angle coverts the two input channels into the HMAX' and Z' channels (Figure 12.26). Once again, the polarization method has been performed on the

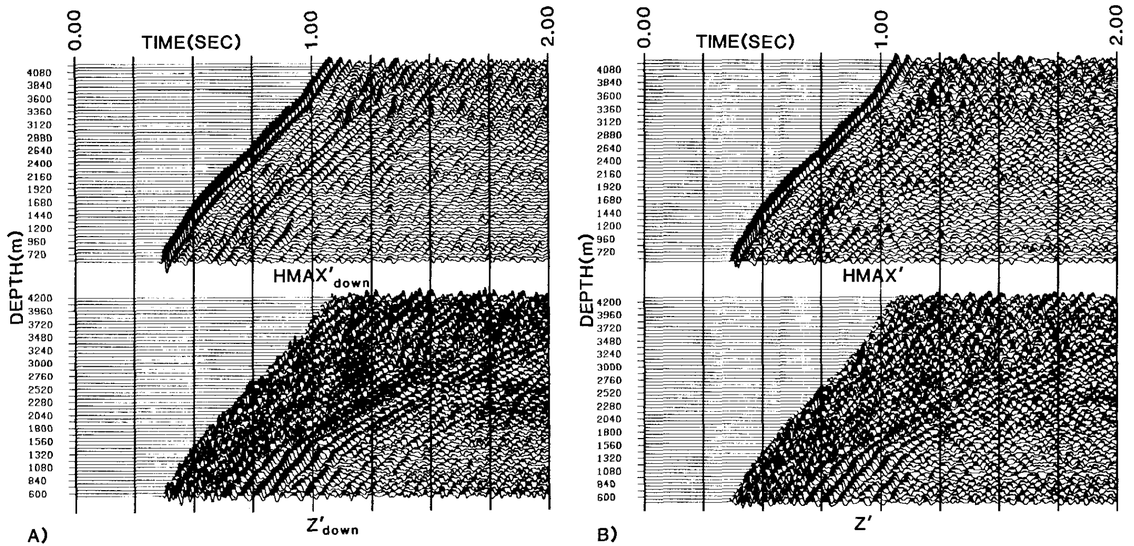

Figure 12.28. After the second downgoing wave first break polarization analysis, the downgoing P and SV wavefields are

downgoing first break energy. On the Z' and HMAX' panels, the upgoing P and SV wavefields are not yet polarized. In order to accomplish this, the time-variant model-based polarization method is used. The IPP which serves as a quality control measure on the usual downgoing P wave first break hodogram analysis is shown in Figure 12.27. On the panel, the degree of success of the downgoing P and

separated from the upgoing P and SV wavefields on the Z' and HMAX' data. The panels show the Z'_{down} and $HMAX'_{down}$ data.

SV wavefield polarization can be determined by comparing the downgoing waves on the X, Y and Z channels versus on the Z' and HMAX' data.

The downgoing waves, both P and SV, are separated from the Z' and HMAX' data using one of the wavefield separation techniques.

Figure 12.27. The IPP that is a quality control measure for the downgoing P-wave first break based hodogram analysis. The panel consists of the X, Y, Z, HMIN, HMAX, Z' and HMAX' data.

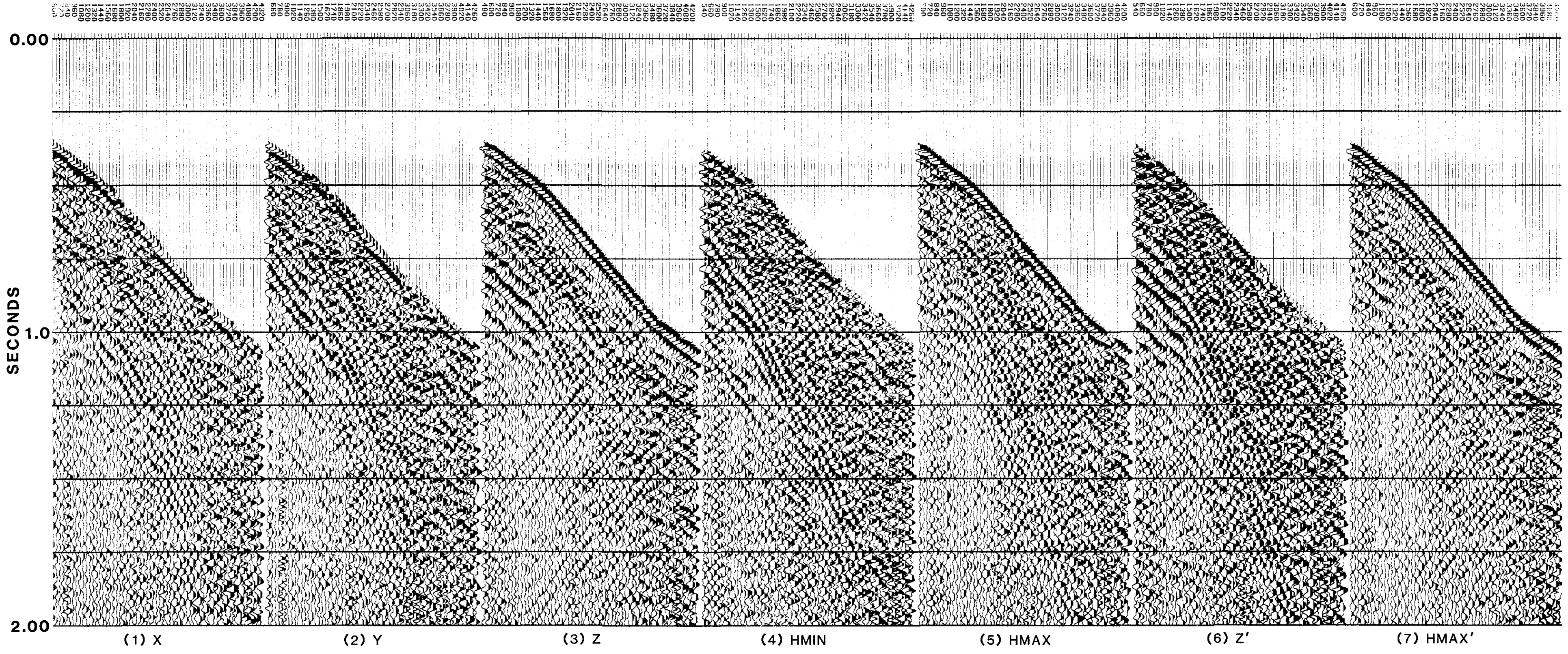

DONOR: GULF CANADA RESOURCES LTD. | PROCESSOR: COMPUTALOG GEARHART LTD. | AUTHOR: R.C. HINDS

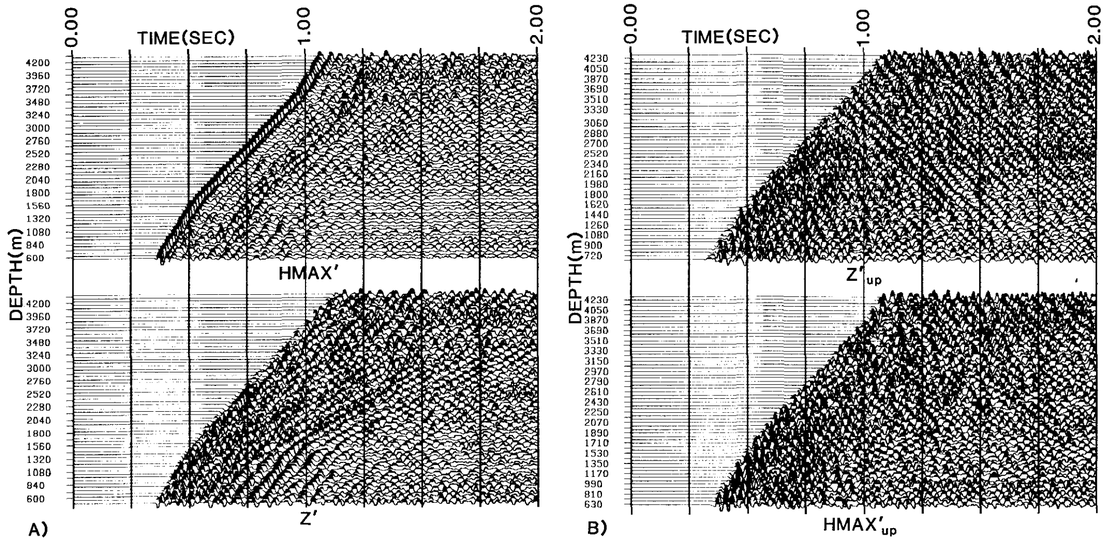

Figure 12.29. After the second downgoing wave first break polarization analysis, the upgoing P and SV wavefields are separated from the downgoing P and SV wavefields on the Z' and HMAX'

The process of up and downgoing wavefield separation applied to the Z' and HMAX' panels result in four new panels, namely Z'_{up}, Z'_{down}, $HMAX'_{up}$ and $HMAX'_{down}$. It is important at this point to keep track of the inputs and outputs to the datasets because of the many algorithms that are being used on the data. The interpreter

data (the two modes are mixed on the two datasets). The panels show the Z'_{up} and $HMAX'_{up}$ data.

cannot simply have faith at this point. The separated downgoing P and SV wavefields from the input Z' and HMAX' channels are shown in Figure 12.28. The mixed upgoing P and SV wavefields (polarized on the downgoing first breaks) in the Z' and HMAX' input panels are shown in Figure 12.29.

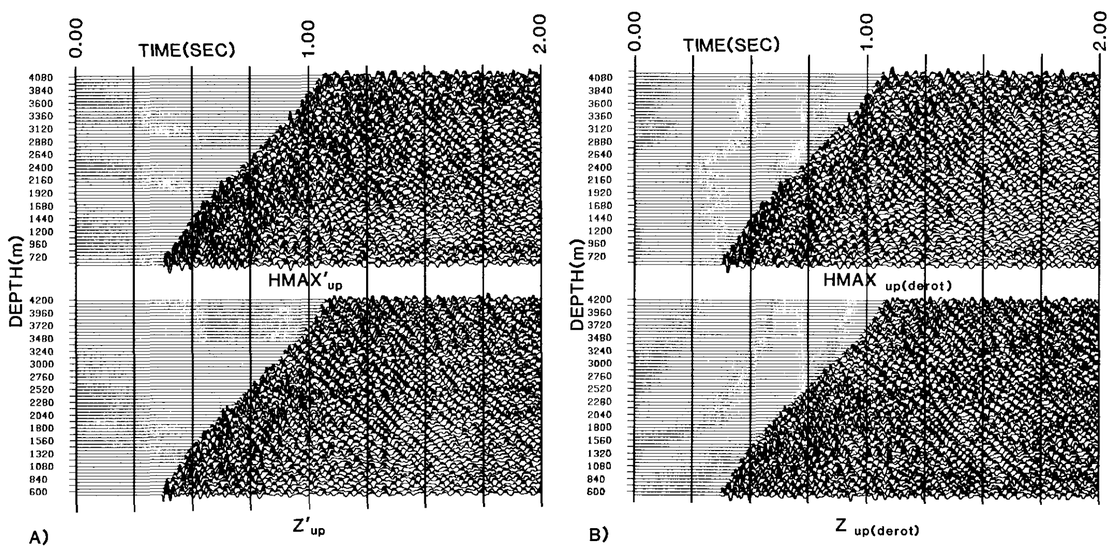

Figure 12.30. The upgoing P and SV isolated waves appearing on both Z_{up} and $HMAX_{up}$ panels (generated by the processing sequence of hodogram analysis on the Z and HMAX data, upgoing wavefield separation on the Z' and HMAX' data and then de-rotating the Z'_{up} and $HMAX'_{up}$ back to the Z_{up} and $HMAX_{up}$ datasets) are not separated in different panels because the hodogram analysis was

At this point, the hodogram-based rotations are reversed in action on the upgoing wavefield panels of the Z' and HMAX' namely

accomplished using the downgoing wave first break region. The input rotated data and de-rotated P and SV upgoing data are shown in part (A) and (B), respectively. Time variant rotation analysis will attempt to isolate the upgoing P and SV wavefields onto the Z'_{up} and $HMAX'_{up}$ channels, respectively.

the Z'_{up} and $HMAX'_{up}$ data. The polarization angle for each trace on the two panels is "backed-out". The result is the Z and HMAX

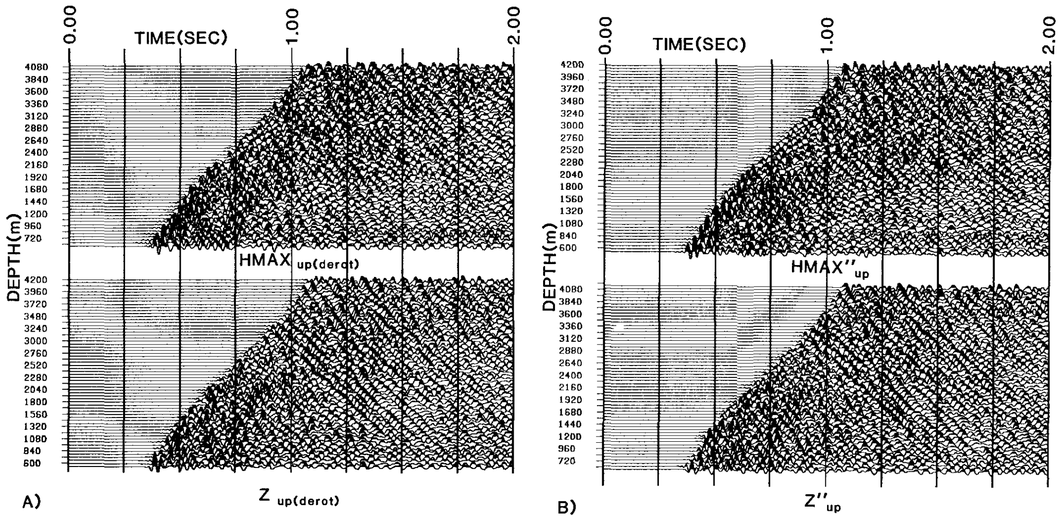

Figure 12.31. The Z_{up} and $HMAX_{up}$ data is rotated using angles derived from the time-variant model-based analysis to form the $Z"_{up}$ and $HMAX"_{up}$ output. The $Z"_{up}$ output is then used for the interpretation of the upgoing P wave and tied to the surface seismic and the well log data.

panels without the downgoing P and SV waves but with the mixed upgoing waves (Z_{up} and $HMAX_{up}$). Note that the P and SV downgoing waves had to be polarized first in the Z' and HMAX' panels before attenuation of those waves took place. The resultant new Z and HMAX panels (Fig. 12.30) will be called the Z_{up} and the $HMAX_{up}$ panels in order to denote that the panels differ with the set of Z and HMAX data previously shown in Figure 12.26.

A velocity model is constructed and input to a Paraxial ray theory-based (Beydoun, 1985) ray-tracing modelling package. This package will estimate the angles at which the upgoing P and SV waves will emerge into the well geophones at the receiver depths with respect to the input two-dimensional velocity model.

The Z_{up} and $HMAX_{up}$ panels are rotated according to the incoming angles of the upgoing P-wave (according to the ray-tracing for the model). The output panels from the polarization, called $Z"_{up}$ and $HMAX"_{up}$ approximate polarized upgoing P and SV, respectively. The input and output channels from the time variant model-based rotations are shown in Figure 12.31.

The dataset shown in this example could be termed as difficult with respect to added noise caused by less than perfect borehole conditions, poor to fair geophone coupling and source placement. This results in data which requires all the IPP displays together to aid in the interpretation. To this end, the IPP for the time-variant rotation is shown on Figure 12.32. The upgoing P wave energy needs to be recognized and interpreted on the datasets and then analysed throughout the panels to ensure that contamination to the data did not occur.

The upgoing shear wave may not be completely polarized into the $HMAX"_{up}$ channel. Another step of the time-variant (model-based) polarization analysis could be done.

VSPCDP TRANSFORMATIONS

In order to reasonably image the subsurface at the zone of interest away from the borehole, the VSPCDP transform is used to convert the LSP data axis from depth and +TT time to offset away from the well and "migrated +TT time". As shown in Figure 12.33, the image points of upgoing wave energy reflecting from horizontal layers of equal or different acoustic impedance form a locus curve. The VSPCDP transform takes the traces recorded at the different depths and, using an input velocity-depth function, stretches the traces over individual locus curves. The curves are regrouped into trace format by a "mapping" or "binning" procedure. The horizontal axis is now offset away from the well.

INTERPRETATION

The VSPCDP transform has imaged the data from 0 to 500 m away from the wellbore. The events from 300 to 1000 ms may be spatially aliased (visually smeared) due to the stretching of the traces over the locus curves and then the resultant binning (or regrouping) back into trace format. The interpreted events are the Nordegg,

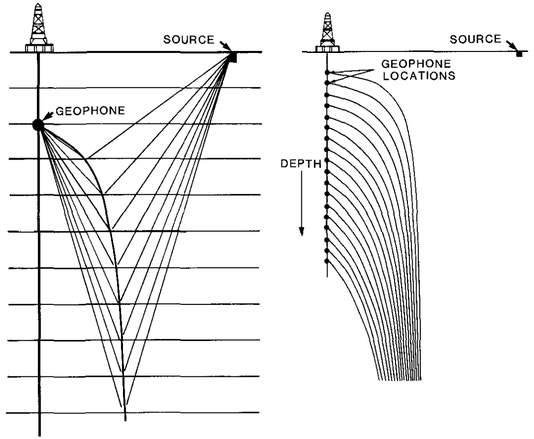

Figure 12.33. The VSPCDP transform locus curve. For this pseudo-migration, the dataset is shifted spatially to a new horizontal axis, being offset away from the well (after Dillon and Thomson, 1984).

Wabamun, Ireton, Westerdale, Duvernay and Cooking Lake along with the postulated near-Cambrian event. The IPP in Figure 12.34 shows the $Z"_{up}$ data in pseudo two-way travel-time. One can note the P and SV downgoing and "extra" upgoing SV contamination. The upgoing SV wave energy theoretically should be primarily polarized into the $HMAX"_{up}$ data but due to violations of the assumptions by the data in the polarization analysis, some of the upgoing SV data "leaks" into the $Z"_{up}$ data. When the SV energy is filtered out of the $Z"_{up}$ data, the effect of the filtering on the resultant upgoing P wave data must be given consideration during the interpretation. Usually, the downgoing SV energy will be of larger amplitude than the upgoing P energy and, as a result of the SV wave separation from the $Z"_{up}$ data, the P wave events will suffer destructive interference (dim spots) where the SV data had previously crossed the combined wavefield dataset. The resultant VSPCDP of the $Z"_{up}$ filtered data may be less continuous than expected.

The VSPCDP of the $Z"_{up}$ data in Figure 12.34 shows that:

Figure 12.32. The IPP for the time-variant model-based rotations showing the separated upgoing P and SV mixed wavefield panels after the second downgoing P-wave first break based hodogram rotations, the same two panels after the backing out of the second hodogram rotations and the resultant Z''_{up} and $HMAX''_{up}$ after the time-variant rotations are applied. The Z''_{up} panel is median filtered and placed into offset away from the well and two-way traveltime coordinates (Fig. 12.34) using the VSPCDP transformation to enable a final interpretation.

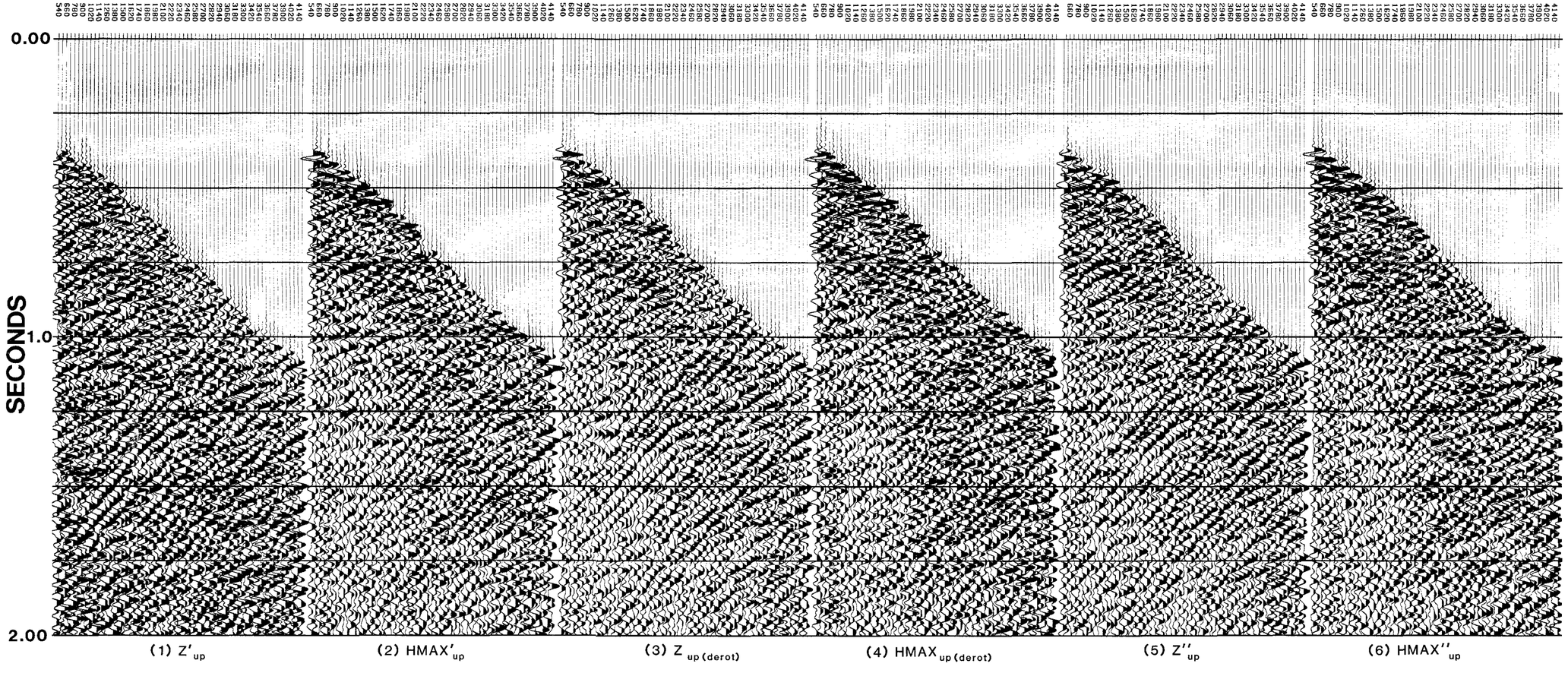

DONOR: GULF CANADA RESOURCES LTD. | PROCESSOR: COMPUTALOG GEARHART LTD. | AUTHOR: R.C. HINDS

Figure 12.34. The Interpretive Processing Panel for the $Z^{"}_{up}$ and the VSPCDP in normal and reverse polarity. The IPP contains the input data and the transformed data allowing a visual check on the VSPCDP transformation. The Ireton Fm, Westerdale Limestone and Duvernay Fm are continuous and flat lying indicating that the edge of the reef has not been imaged for at least 450 m in the direction of the LSP offset.

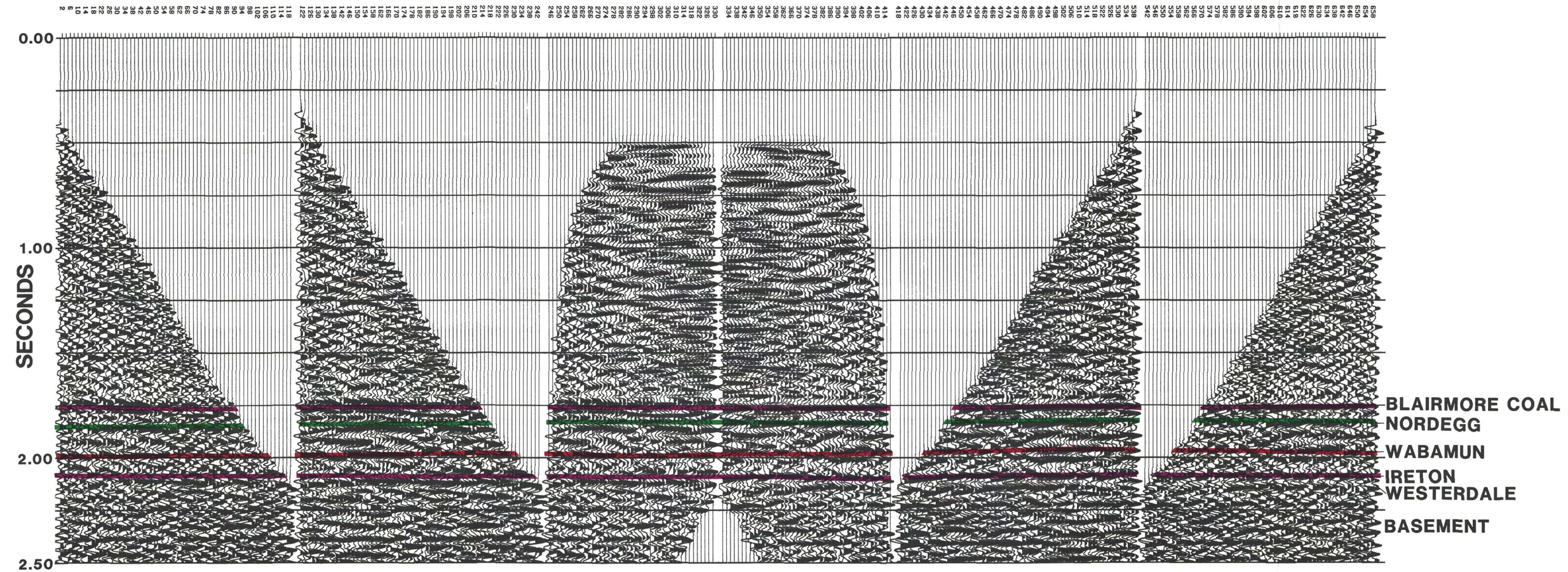

DONOR: GULF CANADA RESOURCES LTD. | PROCESSOR: COMPUTALOG GEARHART LTD. | AUTHOR: R.C. HINDS

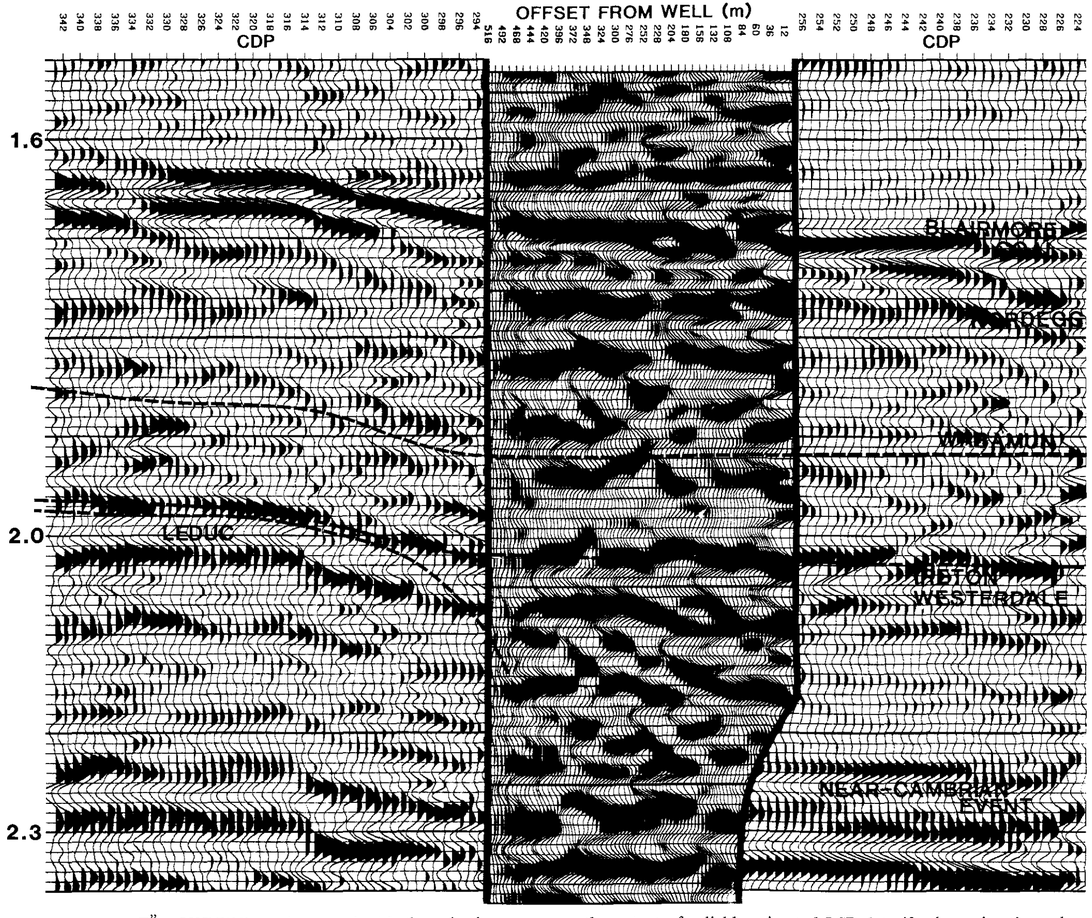

Figure 12.35. The Z''_{up} VSPCDP result merged with the seismic data. The VSPCDP shows that the reef edge is further than 450 m to the west. The areal limits of the VSPCDP can be used to constrain the extent of reliable migrated LSP data if other migration schemes are used on the same dataset.

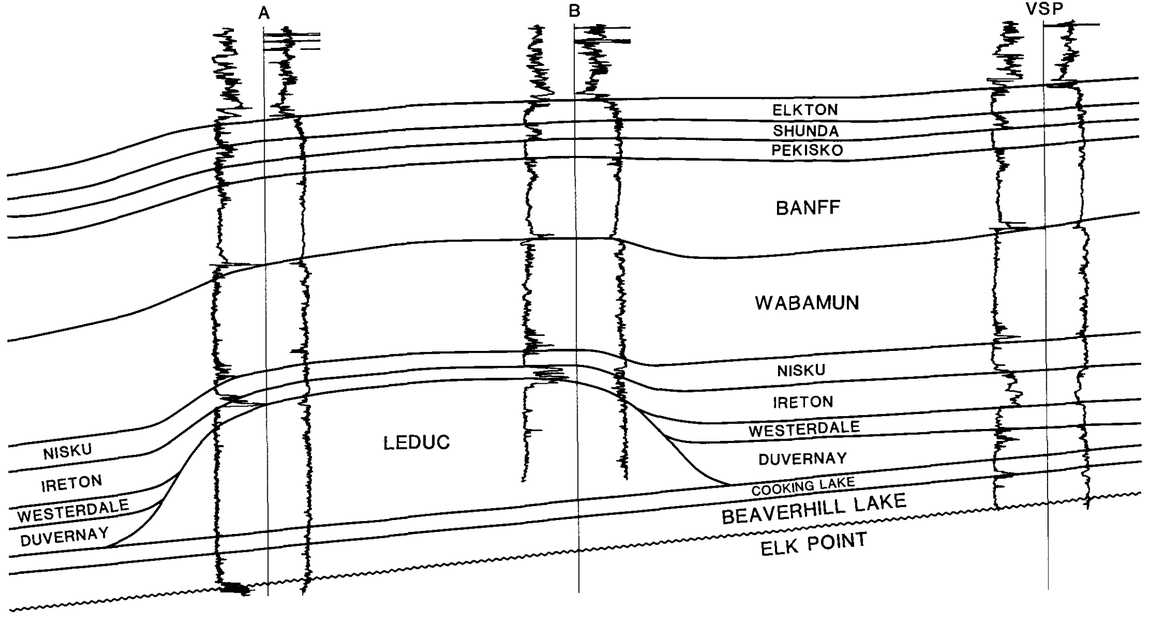

Figure 12.36. The updated geological cross-section incorporating the VSP well log results and the interpreted LSP results. The updip edge of the reef terminates at least 450 m away from the VSP/LSP well.

1) the Ireton Fm, Westerdale Limestone and Duvernay Fm events are continuous and do not resemble Ireton Fm to reef platform isochron thickening;

2) in the opposite polarity plots, the Westerdale Limestone is continuous and does not truncate as would be expected if the reef edge had been encountered;

3) there is no apparent drape features towards the reef exhibited on the Viking and Nordegg formations or Wabamun Gp; and

4) there is no apparent pull-up displayed by the near-Cambrian event (between the Wabamun Gp and the near-Cambrian event) across the LSP section.

The VSPCDP LSP results can be merged into the seismic data as is shown in Figure 12.35. The interpretation of the LSP shows that the reef edge is beyond the 450 m distance in the interpreted reef direction. The reinterpreted surface seismic data along with the post-drilling LSP interpretation aided the redesign of the geological cross-section of well A, B and the VSP well shown in Figure 12.36.

CONCLUSIONS

This chapter has presented the logic and displays used to maximize the amount of information that can be derived from a VSP or LSP. The interpretation was shown to be intimately linked to the evaluation of the various processing steps.

The Lanaway/Garrington VSP enabled the surface seismic interpreter to better understand both the isochron and amplitude anomaly on the surface seismic. The Ricinus VSP enabled a redefined higher resolution interpretation of the surface seismic at the well location plus an evaluation of the effect of multiples on the Wabamun seismic marker. The LSP interpretation showed that the off-reef seismic markers extended to a distance up to 450 m away from the borehole.

VSP and LSP surveys when performed with specific exploration objectives in mind can produce high resolution results that will further minimize the risk of drilling non-profitable oil and gas wells.

REFERENCES

Balch, A.H. and Lee, M.W. (eds), 1984. Vertical Seismic Profiling, Technique, Applications and Case Histories, IHRDC, 488 p.

Balch, A.H., Miller, J.J.,Lee, M.W. and Ryder, R.T. 1981, Processed and interpreted US Geological Survey seismic reflection profile and vertical seismic profile, Powder River and Custer counties, Montana: USGS Chart OC-108.

Beydoun,W.B. 1985. Asymptotic wave methods in heterogeneous media: Ph.D. thesis, Massachusetts Institute of Technology, Cambridge, Massachusetts.

Dillon, B.P. and Thomson, R.C. 1984. VSP surveys and their image reconstruction. Geophysical Prospecting, v. 32, p. 790-811.

Hardage, B.A. 1983. Vertical Seismic Profiling, Part A: Principles, Geophysical Press, London.

Kennett, P., Ireson, R.L. and Conn, P.J. 1980. Vertical seismic profiles – their applications in exploration geophysics; Geophysical Prospecting, v. 28, p. 676-699.

Lee, M.W., Miller, J.J., Ryder, R.T. and Balch, A.H. 1981. Processed and interpreted US Geological Survey seismic reflection profile and vertical seismic profiles, Niobrara County, Wyoming: US Geological Survey Oil and Gas Investigations Chart OC-114.